

Boussinesq–Green–Naghdi rotational water wave theory

Yao Zhang ^a, Andrew B. Kennedy ^{a,*}, Nishant Panda ^b, Clint Dawson ^b, Joannes J. Westerink ^a

^a Department of Civil & Environmental Engineering & Earth Sciences, University of Notre Dame, Notre Dame, IN 46556, USA

^b Department of Aerospace Engineering and Engineering Mechanics, the University of Texas at Austin, 210 East 24th Street, W.R. Woolrich Laboratories, 1 University Station, C0600 Austin, TX 78712-0235, USA

ARTICLE INFO

Article history:

Received 4 March 2012

Received in revised form 14 September 2012

Accepted 17 September 2012

Available online xxxx

Keywords:

Water waves

Boussinesq equations

Computational methods

ABSTRACT

Using Boussinesq scaling for water waves while imposing no constraints on rotationality, we derive and test model equations for nonlinear water wave transformation over varying depth. These use polynomial basis functions to create velocity profiles which are inserted into the basic equations of motion keeping terms up to the desired Boussinesq scaling order, and solved in a weighted residual sense. The models show rapid convergence to exact solutions for linear dispersion, shoaling, and orbital velocities; however, properties may be substantially improved for a given order of approximation using asymptotic rearrangements. This improvement is accomplished using the large numbers of degrees of freedom inherent in the definitions of the polynomial basis functions either to match additional terms in a Taylor series, or to minimize errors over a range. Explicit coefficients are given at $O(\mu^2)$ and $O(\mu^4)$, while more generalized basis functions are given at higher order. Nonlinear performance is somewhat more limited as, for reasons of complexity, we only provide explicitly lower order nonlinear terms. Still, second order harmonics may remain good to $kh \approx 10$ for $O(\mu^4)$ equations. Numerical tests for wave transformation over a shoal show good agreement with experiments. Future work will harness the full rotational performance of these systems by incorporating turbulent and viscous stresses into the equations, making them into surf zone models.

© 2012 Elsevier B.V. All rights reserved.

1. Introduction

Modern Boussinesq water wave theory began in the 1960s as moderate computing power became more available to researchers. Papers by Peregrine (1967), and Madsen and Mei (1969) extended the shallow water equations asymptotically into deeper water to arrive at inviscid, nonlinear, wave evolution equations with leading order dispersive effects. These were confined to relatively shallow water, with $\mu \equiv k_0 h_0 < 1.5$, where k_0 is a typical wavenumber and h_0 is a typical water depth and so had a limited range of application. However, even at these early stages it was realized that entire families of equations could be developed that were asymptotically identical but had differing properties. With exceptions (Witting, 1984), this finding was largely ignored until the early 1990s when several groups of researchers (Madsen and Sørensen, 1992; Madsen et al., 1991; Nwogu 1993) used various methods of asymptotic rearrangement to improve properties of Boussinesq equations so that dispersion relations were accurate to the nominal deep water limit of $k_0 h_0 \approx \pi$. Further work increased nonlinearity from the mildly nonlinear equations that existed previously to so-called fully nonlinear equations with considerably more accurate nonlinear properties (Kennedy et al.,

2001; Madsen and Schäffer, 1998; Wei et al., 1995). Formal expansions to higher order increased the accuracy of all properties (Gobbi and Kirby, 1999; Gobbi et al., 2000; Madsen and Schäffer, 1998) but at the cost of much more complex equations. Extensions to include wave breaking and shorelines have made these into true surf zone models able to represent waves and wave-induced currents including wave setup, rip currents, and longshore currents (e.g. Bonneton et al., 2011a; Chen et al., 2000; Kennedy et al., 2000a,b; Lynett, et al., 2002; Nwogu and Demirbilek, 2010; Schäffer and Madsen, 1993; Sørensen et al., 1998).

However, there were obstacles to this progress. It was discovered (Kennedy and Kirby, 2002; Madsen and Agnon, 2003) that the basic asymptotic series underlying the velocity structure was only conditionally convergent, and diverged strongly for higher order equations at moderate wavenumbers. This finding, along with the highly complex nature of higher order equations, led to a stagnation in some parts of Boussinesq theory. Partial solutions have been found: convergent formulations of very high order have been derived and tested (Lynett and Liu, 2004; Madsen and Agnon, 2003; Schäffer, 2009); however, the extension of these irrotational formulations to true rotational surf zone models has not been immediately forthcoming. This partial or full irrotationality assumption for orbital velocities is present in almost all Boussinesq models, and represents a second obstacle to progress. While appropriate for nonbreaking waves, these assumptions are strongly violated in the surf zone. Again, this has been addressed on multiple occasions using

* Corresponding author.

E-mail address: andrew.kennedy@nd.edu (A.B. Kennedy).

irrotational/rotational decompositions with different scalings (Musumeci et al., 2005; Shen, 2001; Veeramony and Svendsen 2000) but only at lower order, and often with vertical vorticity specified instead of arising naturally. None of these approaches has been widely adopted, which is unfortunate as surf zone simulations require the inclusion of vorticity to provide accurate reconstructions of internal velocities.

Taken together, these limitations have hindered investigations into processes like sediment transport, where Boussinesq models had been expected to excel. Still, prediction of nonlinear water surface elevations and bulk currents in and around the surf zone remains good, and existing models are very useful.

An alternate but related approach to the computation of shallow water nonlinear dispersive waves lies in the Green–Naghdi or Serre approach (Bonneton et al., 2011a,b; Green and Naghdi, 1976; Serre, 1953; Shields and Webster, 1988). Here, a polynomial structure is also retained for the velocity profile. In the original approach of Green and Naghdi, no irrotationality constraint is applied, and no scaling or perturbation parameters are used. A finite series of velocities is substituted into the mass and momentum equations and solved in a weighted residual sense. Rotational Green–Naghdi equations have shown excellent nonlinear properties and very fast convergence with increasing numbers of terms in the series (Shields and Webster, 1988). However, their extreme complexity in addition to their lack of formal asymptotic justification has meant that they are rarely used at higher order: almost all implementations of rotational Green–Naghdi theory have been at low levels of approximation (e.g. Ertekin et al., 1986). More recently, researchers have introduced irrotational characteristics and scaling into Green–Naghdi theory (e.g. Bonneton et al., 2011a,b; Lannes and Bonneton, 2009), which brings it more in line with standard Boussinesq systems, and recent advances have improved dispersion considerably (Lannes and Bonneton, 2009). Again, these improvements tend to be at $O(\mu^2)$ although linear dispersion may be considerably more accurate.

Alternate polynomial summation representations assuming irrotational flow (Kennedy and Fenton, 1997; Kim et al., 2003) have no difficulties with higher order series, and have demonstrated extremely high accuracy with implementation to arbitrary order for nonbreaking waves; however their fundamentally irrotational formulations preclude even ad hoc extension to surf zones. Thus there remains considerable opening for formulations incorporating vorticity that have good linear and nonlinear properties.

Here, we derive and test systems of equations for nonlinear water wave transformation. Like Green–Naghdi systems, we use polynomial expansions (Shields and Webster, 1988), but also employ Boussinesq scaling; however the present derivation is without the partial or complete irrotationality assumption of most Boussinesq systems so that rotational surf zone flows may be modeled naturally. The systems may be extended to higher order and show excellent convergence towards exact solutions for dispersion, shoaling, and orbital velocities. The end results show a resemblance to both Boussinesq and Green–Naghdi systems, and may be recast into different forms. Importantly, most of the asymptotic rearrangement techniques used for Boussinesq models may also be employed here to improve accuracy for given levels of approximation.

The present paper introduces these systems, examines their properties, and provides introductory numerical results. For this first paper, we concentrate only on inviscid properties and numerical tests and thus neglect the turbulent/viscous stresses which are important in the surf and swash zones. These will prove to be essential in extending the applicability of the model and taking advantage of its rotational capabilities, but are best developed and evaluated in separate publications. Future papers will thus extend the systems developed here for surf zone use, and describe their detailed numerical solution methods.

2. Scaling

Boussinesq-shallow water scaling for non-dimensional variables is:

$$\begin{aligned} (x, y) &= k_0(x^*, y^*), \quad z = h_0^{-1}z^*, \quad t = k_0(g h_0)^{1/2}t^*, \quad h = h_0^{-1}h^*, \quad \eta = (h_0)^{-1}\eta^* \\ P &= (\rho^* g_0 h_0)^{-1}P^*, \quad g = g_0^{-1}g^*, \quad (u, v) = (g_0 h_0)^{-1/2}(u^*, v^*), \quad w = (k_0 h_0)^{-1}(g_0 h_0)^{-1/2}w^* \end{aligned} \quad (2.1)$$

where the superscript * indicates a dimensional variable. Horizontal coordinates are (x^*, y^*) and the vertical coordinate z^* is oriented upward. Time t^* is scaled based on a long wave speed and wavelength, while depth h^* and surface elevation η^* scale with typical water depth. The pressure P^* scales hydrostatically in long wave theory where g^* is gravitational acceleration. Horizontal and vertical fluid velocities (u^*, v^*, w^*) all scale with wave orbital velocities taken from shallow water theory. There is an implicit assumption in this scaling that the wave may be strongly nonlinear, although of course the system is also valid for small amplitude waves.

Although this will be relaxed in the future, for the present paper we will assume flow with no turbulent/viscous stresses. These stresses will be necessary for surf zone processes and for computation of velocity profiles in steady flows, but are not necessary for the present derivations and tests. We also note that the inclusion of viscous forces will introduce another set of velocity and pressure scaling parameters which will become important in some situations.

When inserted into the continuity equation, kinematic free surface, and bottom boundary conditions, dimensionless equations become

$$\nabla \cdot \mathbf{u} + \frac{\partial w}{\partial z} = 0, \quad -h \leq z \leq \eta \quad (2.2)$$

$$w = -\mathbf{u} \cdot \nabla h, \quad z = -h \quad (2.3)$$

$$w = \frac{\partial \eta}{\partial t} + \mathbf{u} \cdot \nabla \eta, \quad z = \eta \quad (2.4)$$

where $\nabla \equiv (\partial/\partial x, \partial/\partial y)$, $\mathbf{u} = (u, v)$. Integrating Eq. (2.2) from bottom to surface and applying kinematic boundary conditions gives a mass equation in conservation form,

$$\frac{\partial \eta}{\partial t} + \nabla \cdot \int_{-h}^{\eta} \mathbf{u} dz = 0 \quad (2.5)$$

The three dimensional momentum equations for incompressible, inviscid fluid motion are

$$\frac{\partial \mathbf{u}}{\partial t} + \mathbf{u} \cdot \nabla \mathbf{u} + w \frac{\partial \mathbf{u}}{\partial z} + \nabla P = 0 \quad (2.6)$$

$$\mu^2 \frac{\partial w}{\partial t} + \mu^2 \mathbf{u} \cdot \nabla w + \mu^2 w \frac{\partial w}{\partial z} + \frac{\partial P}{\partial z} + g = 0 \quad (2.7)$$

Integrating Eq. (2.7) from z to η , and assuming a zero gauge pressure at the free surface, we find

$$P(z) = \mu^2 \int_z^{\eta} \frac{\partial w}{\partial t} dz + \mu^2 \int_z^{\eta} \mathbf{u} \cdot \nabla w dz + \mu^2 \int_z^{\eta} w \frac{\partial w}{\partial z} dz + g(\eta - z) \quad (2.8)$$

So far these equations are quite general. An implicit assumption that both the free surface and bed have single-valued elevations is shared by all Boussinesq-type and Green–Naghdi wave models. This assumption is excellent outside the surf zone but may be strongly violated in the case of plunging breakers, which will have at least three air-water interfaces on the plunging jet. Because of this, there will be

an upper limit to accuracy imposed by the single valued assumption. This must be kept in mind as the derivation proceeds: at some point (where is not entirely clear) an increasing level of approximation will cease to bring a commensurate increase in accuracy once the surf zone is encountered. For this reason, moderate levels of approximation may prove to be the optimal combination of accuracy and efficiency for some problems.

2.1. Velocity expansion

Classical Boussinesq theory assumes a polynomial expansion for the horizontal velocity

$$\mathbf{u} = \sum_{n=0}^{\infty} \tilde{\mathbf{u}}_n(x, y, t)(z + h)^n \tag{2.9}$$

where the infinite series is in practice truncated to a desired level of approximation. When substituted into the continuity Eq. (2.2), bottom boundary condition (2.3), and a partial irrotationality condition (which will not be used here), the lowest order solution corresponds to the bottom velocity, $\tilde{\mathbf{u}}_0$. Successive recursions then give higher order horizontal and vertical velocity components as higher derivatives of the bottom velocity, $\tilde{\mathbf{u}}_0$. As Boussinesq equations based on the bottom velocity have poor properties, these may be asymptotically rearranged into other forms: for example the velocity formulation of Nwogu (1993) has, in the present scaling,

$$\mathbf{u} = \mathbf{u}_\alpha + \mu^2(z_\alpha - z)\nabla(\nabla \cdot (h\mathbf{u}_\alpha)) + \mu^2\left(\frac{z_\alpha^2}{2} - \frac{z^2}{2}\right)\nabla(\nabla \cdot \mathbf{u}_\alpha) + O(\mu^4) \tag{2.10}$$

where the new reference velocity \mathbf{u}_α is defined at $z = z_\alpha(x, y, t)$. With the usual definition of $z_\alpha \equiv \hat{C}h$, where \hat{C} is a free constant of $O(1)$, the horizontal velocity may be reduced to

$$\begin{aligned} \mathbf{u} &= \underbrace{\hat{\mathbf{u}}_0}_{\mathbf{u}_\alpha} + \underbrace{\mu^{\beta_1} \overbrace{\left(\left(\hat{C} + 1\right) - \frac{z+h}{h}\right)}^{f_1}}_{\mu^2} \underbrace{\hat{\mathbf{u}}_1}_{h[\nabla(h\nabla \cdot \mathbf{u}_\alpha) + \nabla(\mathbf{u}_\alpha \cdot \nabla h)]} \\ &+ \underbrace{\mu^{\beta_2} \overbrace{\frac{1}{2}\left(\left(\hat{C} + 1\right)^2 - \left(\frac{z+h}{h}\right)^2\right)}^{f_2}}_{\mu^2} \underbrace{\hat{\mathbf{u}}_2}_{h^2\nabla(\nabla \cdot \mathbf{u}_\alpha)} + O(\mu^4) \\ &= \sum_{n=0}^N \mu^{\beta_n} \hat{\mathbf{u}}_n(\mathbf{x}) \hat{f}_n \end{aligned} \tag{2.11}$$

where, for consistency with Nwogu $N=2$, but this representation could be generalized to any even number for an $O(\mu^4)$ or higher order velocity field. The velocity scaling $\beta_n = n$ when n is even, and $n + 1$ when n is odd. The polynomial functions \hat{f}_n are functions of $(z + h)/h$, include components up to $((z + h)/h)^n$, and thus the polynomial degree increases with n . Polynomial coefficients and velocities $\hat{\mathbf{u}}_n$ arise from two sources: (1) the definition of the reference elevation, z_α , and (2) the combination of irrotationality, continuity and bottom boundary conditions that allow higher order velocities to be represented as functions of lowest order velocity, \mathbf{u}_α .

There is one further useful rearrangement here: if we define the reference elevation to be a constant fraction of the total water depth, i.e. $z_\alpha = -h + (\hat{C} + 1)(h + \eta)$, the reference elevation will have no dependence on the definition of the zero datum and tide level, which is a useful property (e.g. Kennedy et al., 2001). This may be represented more naturally by the vertical coordinate $q \equiv (z + h)/(h + \eta)$ and thus $q_\alpha \equiv (z_\alpha + h)/(h + \eta) = \hat{C} + 1$. This q is a coordinate that varies between zero at the bed and one at the free

surface, and is simply a sigma coordinate plus one. With these definitions, Nwogu's velocities become

$$\begin{aligned} \mathbf{u} &= \underbrace{\hat{\mathbf{u}}_0}_{\mathbf{u}_\alpha} + \underbrace{\mu^{\beta_1} \overbrace{\left(\left(\hat{C} + 1\right) - \frac{z+h}{h}\right)}^{f_1}}_{\mu^2} \underbrace{\hat{\mathbf{u}}_1}_{h[\nabla(h\nabla \cdot \mathbf{u}_\alpha) + \nabla(\mathbf{u}_\alpha \cdot \nabla h)]} \\ &+ \underbrace{\mu^{\beta_2} \overbrace{\frac{1}{2}\left(\left(\hat{C} + 1\right)^2 - \left(\frac{z+h}{h}\right)^2\right)}^{f_2}}_{\mu^2} \underbrace{\hat{\mathbf{u}}_2}_{h^2\nabla(\nabla \cdot \mathbf{u}_\alpha)} + O(\mu^4) \end{aligned} \tag{2.12}$$

$$\mathbf{u} = \sum_{n=0}^N \mu^{\beta_n} \mathbf{u}_n(\mathbf{x}) f_n \tag{2.13}$$

In the derivations to follow, we wish to be able to represent rotational flows and thus abandon irrotationality. Thus, we will define velocities using Eq. (2.13) and with arbitrary even N (which will produce a system complete up to $O(\mu^N)$); however, unlike Nwogu, all horizontal velocities $\mathbf{u}_0, \mathbf{u}_1, \dots, \mathbf{u}_N$ are independent, which is a fundamental difference between irrotational and rotational flows. Finally, we allow arbitrary constants for polynomial coefficients. To ensure a consistent solution that is in accordance with Boussinesq scaling, polynomial functions $f_n(q)$ must have the form $f_n = \sum_{m=0}^n a_{nm} q^m$, where a_{nm} are real constants with $a_{nn} \neq 0$. It is assumed without loss of generality that $f_0 = 1$. Specification of both the order of approximation, $O(\mu^N)$, and the polynomial coefficients, a_{nm} , will define the specific systems once substituted into the mass and momentum equations. In particular, different choices of a_{nm} will yield different wave properties through asymptotic rearrangement in a manner that is like the change in properties given by using different reference velocities in Nwogu (1993).

These decoupled velocities form the basis of rotational Green–Naghdi type systems, and immediately lead to major differences since higher order velocity components are not defined in terms of lower order components. The vertical velocity, w , is then uniquely specified from the continuity equation and bottom boundary condition as

$$w = \sum_{n=0}^N \mu^{\beta_n} [-(\nabla \cdot \mathbf{u}_n)(h + \eta)g_n + (\mathbf{u}_n \cdot \nabla(h + \eta))r_n - (\mathbf{u}_n \cdot \nabla h)f_n] \tag{14}$$

where g_n and r_n are integral functions of f_n , e.g. $g_n \equiv \int f_n(q) dq$, with many other functions defined in Table 1. All integrals have constant of integration defined such that $g_n|_{q=0} = 0$ and thus $g_n|_q^1 = g_n|_{q=1}$. The velocity expansions are inserted into the mass and momentum equations and terms are kept or discarded according to the assumed order of approximation, $O(\mu^N)$. It should be noted that the definitions of basis functions will thus influence the form of the velocities here in the same way as the definition of z_α affects velocities in Nwogu's equations. This influence carries over into the dynamical systems, where entire families of equations may be developed that are asymptotically identical to the order of approximation, but have different overall properties.

3. Boussinesq–Green–Naghdi Water Wave Systems

Given scaled initial velocity fields, surface elevation defined over the entire fluid domain, and a desired level of approximation, the

Table 1

Integral definitions used in this paper. All indefinite integrals will be assumed to have integration constants defined to give values of 0 at $q = 0$. Thus, for example, $g_n|_q^1 = g_n|_{q=1}$.

| | | |
|--|---------------------------------|---------------------------------|
| $g_n = \int f_n dq$ | $r_n = \int f_n q dq$ | $G_n = \int g_n dq$ |
| $R_n = \int r_n dq$ | $\phi_{mn} = \int f_m f_n dq$ | $\gamma_{mn} = \int f_m g_n dq$ |
| $\rho_{mn} = \int f_m r_n dq$ | $\Gamma_{mn} = \int f_m G_n dq$ | $\Theta_{mn} = \int f_m R_n dq$ |
| $\theta_{mn} = \int f_m g_n q dq$ | $\nu_m = \int q^2 f_m dq$ | $S_m = \int q f_m dq$ |
| $\varepsilon_{mn} = \int f_m f_n q dq$ | $\Psi_{mn} = \int f_m r_n q dq$ | $F_{mn} = \int f_m r_n q dq$ |

only equations left to be satisfied are the free surface evolution Eq. (2.5), the momentum Eq. (2.6), and the pressure Eq. (2.8). For all systems, generalities of the solution method are the same, but details will differ according to the level of approximation and basis functions chosen.

1. Define a desired level of wave approximation, $O(\mu^N)$,
2. Insert velocity field into free surface evolution Eq. (2.5), retaining all terms to specified level of approximation, and discarding all terms that are formally $O(\mu^{N+2})$ or higher.
3. Insert velocity field into pressure Eq. (2.8), retaining all terms to specified level of approximation, and discarding all terms that are formally small.
4. Insert velocity field and expression for pressure into horizontal momentum Eq. (2.6), retaining all terms to specified level of approximation, and discarding all terms that are formally small. Integrate in weighted residual sense as shown in Eq. (3.1) using the $N+1$ basis functions as weights.

$$\int_{-h}^{\eta} f_m \left(\frac{\partial \mathbf{u}}{\partial t} + \mathbf{u} \cdot \nabla \mathbf{u} + w \frac{\partial \mathbf{u}}{\partial z} + \nabla P \right) dz = 0, \quad m = [0, N] \quad (3.1)$$

These systems will, depending on the level of approximation, be able to represent many linear and nonlinear water wave phenomena in depths that are not too large. Unlike standard Boussinesq expansions, rotational processes are included and evolve naturally once turbulent stresses are specified (although they will not be included in this introductory paper). As will be shown, the systems resemble coupled lower order Boussinesq equations, and no mixed space/time derivatives higher than $u_{n,xt}$ will appear, no matter the level of approximation. Although we do not have explicit proofs, the systems appear to converge with increasing order of approximation and do not exhibit the divergence for finite wavenumbers found in many Boussinesq expansions (Kennedy and Kirby, 2002; Madsen and Agnon, 2003). Computational cost for lower order systems will be comparable to existing Boussinesq equations, but higher order systems will of course be more expensive.

Perhaps most importantly, the systems may employ asymptotic rearrangement through the specification of polynomial basis functions f_n . In this, we may build upon the past decades of experience to produce systems of equations with highly accurate linear dispersion and shoaling relations but a relatively low order of formal approximation.

3.1. $O(\mu^2)$ Equations

The lowest level of dispersive approximation is to $O(\mu^2)$ and thus $N=2$. This is further the only level that can be easily derived and coded by hand including all nonlinearities. For all levels of approximation we can without loss of generality define $f_0=1$. The Boussinesq-scaled velocity field is then

$$\begin{aligned} \mathbf{u} &= \mathbf{u}_0 + \mu^2 \mathbf{u}_1 f_1 + \mu^2 \mathbf{u}_2 f_2 + O(\mu^4) \\ w &= -\nabla \cdot \mathbf{u}_0(\eta+h)q - \mathbf{u}_0 \cdot \nabla h + O(\mu^2) \end{aligned} \quad (3.2)$$

It should be noted that here we do not need to include $O(\mu^2)$ terms in the vertical velocity as all terms in the pressure and momentum equations where w appears are already at minimum $O(\mu^2)$, and so any higher order vertical velocity terms in Eq. (3.2) would be discarded from the final equations.

Insertion of the velocity field (Eq. (3.2)) into the free surface evolution equation immediately gives

$$\eta_t + \nabla \cdot \left(\mathbf{u}_0(\eta+h) + \mu^2 \sum_{n=1}^2 \mathbf{u}_n(\eta+h) g_n \Big|_{q=1} \right) = 0 \quad (3.3)$$

where we again see the integral $g_n \equiv \int f_n(q) dq$. Thus, definition of f_n affects the form of the mass equation through integrals. This type of dependency will be found in many other places, and the various integrals are defined in Table 1. Note that these integrals evaluated at $q=1$ (free surface) are simply numbers that may be precomputed easily and exactly and stored for lookup when necessary.

Insertion of the velocity field into the pressure Eq. (2.8) and integration gives

$$\begin{aligned} P(z) &= g(\eta-z) - \mu^2 \left((\nabla \cdot \mathbf{u}_{0,t})(\eta+h)^2 \frac{1-q^2}{2} + \mathbf{u}_{0,t} \cdot \nabla h(\eta+h)(1-q) \right) \\ &\quad + \frac{\mu^2}{2} (\eta+h)^2 \left[(\nabla \cdot \mathbf{u}_0)^2 - \mathbf{u}_0 \cdot \nabla (\nabla \cdot \mathbf{u}_0) \right] (1-q^2) \\ &\quad - \mu^2 (\eta+h) \mathbf{u}_0 \cdot \nabla (\mathbf{u}_0 \cdot \nabla h)(1-q) \end{aligned} \quad (3.4)$$

Note that at this level of approximation, only u_0 appears in the nonhydrostatic pressure corrections, and particularly, in the mixed $u_{0,xt}$ terms. Higher order velocity terms u_1 and u_2 will appear in the mass and momentum equations but do not affect pressure here.

Insertion of Eq. (3.4) into the depth-integrated, weighted momentum Eq. (3.1) then gives, keeping all terms to $O(\mu^2)$,

$$\begin{aligned} \mathbf{u}_{0,t}(\eta+h) g_m |q=1 + \mathbf{u}_0 \cdot \nabla \mathbf{u}_0(\eta+h) g_m |q=1 + g \nabla \eta(\eta+h) g_m |q=1 \\ + \mu^2 \sum_{n=1}^2 \left(\mathbf{u}_{n,t}(\eta+h) \phi_{mn} - \mathbf{u}_n \eta_t \varepsilon_{mn} \right) |q=1 \\ - \mu^2 \left[\frac{1}{2} \nabla (\nabla \cdot \mathbf{u}_{0,t})(\eta+h)^3 (g_m - \nu_m) + (\nabla \cdot \mathbf{u}_{0,t})(\eta+h)^2 \nabla(\eta+h) g_m \right. \\ \left. + \nabla (\mathbf{u}_{0,t} \cdot \nabla h)(\eta+h)^2 (g_m - S_m) + \mathbf{u}_{0,t} \cdot \nabla h \nabla \eta(\eta+h) g_m \right. \\ \left. - (\nabla \cdot \mathbf{u}_{0,t})(\eta+h)^2 \nabla h S_m \right] |q=1 \\ + \mu^2 \sum_{n=1}^2 \left[(\mathbf{u}_n \cdot \nabla \mathbf{u}_0 + \mathbf{u}_0 \cdot \nabla \mathbf{u}_n)(\eta+h) \phi_{mn} - \mathbf{u}_n \nabla \cdot (\mathbf{u}_0(\eta+h)) \varepsilon_{mn} \right] |q=1 \\ + \mu^2 (\eta+h)^2 \left[(\nabla \cdot \mathbf{u}_0)^2 - \mathbf{u}_0 \cdot \nabla (\nabla \cdot \mathbf{u}_0) \right] (\nabla \eta g_m + \nabla h (g_m - S_m)) |q=1 \\ + \frac{\mu^2}{2} (\eta+h)^3 \nabla \left[(\nabla \cdot \mathbf{u}_0)^2 - \mathbf{u}_0 \cdot \nabla (\nabla \cdot \mathbf{u}_0) \right] (g_m - \nu_m) |q=1 \\ - \mu^2 (\eta+h) \nabla \eta \mathbf{u}_0 \cdot \nabla (\mathbf{u}_0 \cdot \nabla h) g_m |q=1 \\ - \mu^2 (\eta+h)^2 \nabla (\mathbf{u}_0 \cdot \nabla (\mathbf{u}_0 \cdot \nabla h)) (g_m - S_m) \Big|_{q=1} = 0, \quad m = 0, 1, 2 \end{aligned} \quad (3.5)$$

Although the mass equation is explicit, the three coupled momentum equations would seem to need to be solved simultaneously for $u_{0,t}$, $u_{1,t}$, and $u_{2,t}$, which would increase the computational cost. However, if it is realized that mixed space-time derivatives only occur for u_0 (i.e. $u_{0,xt}$ and related terms), this may easily be reduced to a form where $u_{0,t}$ and its mixed derivatives are the only unknowns. To do this, $u_{1,t}$ and $u_{2,t}$ must be eliminated from one momentum equation, say $m=0$. The basic form of the equation will not change, but the integrals will. If we define $\tilde{g}_0 \equiv (g_0 - d_0 g_1 - e_0 g_2) |_{q=1}$, where

$$\begin{aligned} d_0 &= \frac{\phi_{01} \phi_{22} - \phi_{21} \phi_{02}}{\phi_{11} \phi_{22} - \phi_{12} \phi_{21}} \\ e_0 &= \frac{\phi_{11} \phi_{02} - \phi_{01} \phi_{12}}{\phi_{11} \phi_{22} - \phi_{12} \phi_{21}} \end{aligned} \quad (3.6)$$

replacement of g_0 with \tilde{g} and equivalently for all other integrals (e.g. ε_{0n} is replaced with $\tilde{\varepsilon}_{0n}$) will result in a replacement equation for $m=0$ that does not contain $u_{1,t}$ or $u_{2,t}$ terms. This will be in the standard $O(\mu^2)$ Boussinesq form and may be arranged into a tridiagonal matrix for 1D to solve for $u_{0,t}$ using methods that are well known. Velocities $u_{1,t}$ and $u_{2,t}$ will in many numerical representations then be solvable purely locally as the solution of a 2×2 matrix, which is straightforward.

In summary, the three momentum Eq. (3.5) should be modified as follows to increase computational efficiency

1. For the $m=0$ equation, replace all integrals $(-)$ with $(-)$. This will eliminate all $u_{1,t}$ and $u_{2,t}$ terms, and the revised equation may then be solved for $u_{0,t}$ independently of the other equations,
2. Using the $m=1,2$ momentum equations and with known $u_{0,t}$, solve for $u_{1,t}$, and $u_{2,t}$.

It is also very important to note that, if shifted Legendre polynomial basis functions are used, $f_n(q) = P_n^*(q)$, this procedure becomes unnecessary as their excellent orthogonality properties mean that $\int_0^1 f_m f_n dq = 0$, $m \neq n$ and thus $u_{n,t} \phi_{mn}|_{q=1}$ terms only appear on the diagonal in momentum equation n . However, at $O(\mu^2)$ shifted Legendre polynomials are probably not the best solution as their dispersion is not as accurate as might be desired.

3.2. $O(\mu^4)$ and Higher Order Equations

Conceptually, higher order equations are straightforward to develop, but are in practice quite complex. Here, we derive and examine $O(\mu^4)$ and higher order equations, but with full nonlinearity only up to $O(\mu^2)$. Because of the very great complexity, terms at higher orders will be linearized only. Thus, they will look like the nonlinear $O(\mu^2)$ equations of the previous section, with additional higher order linear terms. This is an approximation that will limit nonlinear applicability in deeper waters, but should give good nonlinear results in shallower waters and, in particular, should give quite accurate velocity profiles. In practice it may be possible to include all nonlinearities, but these would need to be generated through numerical summations rather than analytical expressions.

The conservation of mass equation requires little change.

$$\eta_{t,t} + \nabla \cdot (\mathbf{u}_0(\eta + h) + \mu^2 \sum_{n=1}^2 \mathbf{u}_n(\eta + h) g_n|_q = 1 + \sum_{n=3}^N \mu^{\beta_n} \mathbf{u}_n h g_n|_q = 1) = 0 \quad (3.7)$$

The integrated conservation of momentum equations are

$$\begin{aligned} & (\mathbf{u}_{0,t}(\eta + h) + \mathbf{u}_0 \cdot \nabla \mathbf{u}_0(\eta + h) + g \nabla \eta(\eta + h)) g_m|_q = 1 + \mu^2 (\dots) \\ & + \sum_{n=3}^N \mu^{\beta_n} h \mathbf{u}_{n,t} \phi_{mn}|_q = 1 \\ & - \sum_{n=1}^{N-2} \mu^{\beta_n} [h \nabla (h^2 \nabla \cdot \mathbf{u}_{n,t}) (G_n|_q = 1 g_m|_q = 1 - \Gamma_{mn}|_q = 1) \\ & - h^2 \nabla \cdot \mathbf{u}_{n,t} \nabla h (\gamma_{mn}|_q = 1 - \theta_{mn}|_q = 1) \\ & + h \nabla (h (\mathbf{u}_{n,t} \cdot \nabla h)) ((g_n - R_n)|_q = 1 g_m|_q = 1 - \gamma_{mn}|_q = 1 + \theta_{mn}|_q = 1) \\ & + h (\mathbf{u}_{n,t} \cdot \nabla h) \nabla h (\rho_{mn}|_q = 1 - F_{mn}|_q = 1 - \phi_{mn}|_q = 1 \\ & + \Psi_{mn}|_q = 1)] = 0, \quad m = [0, N] \end{aligned} \quad (3.8)$$

where $\mu^2(\dots)$ is shorthand for all $O(\mu^2)$ terms in Eq. (3.5). These equations will thus provide the same level of nonlinear approximation as the fully nonlinear $O(\mu^2)$ equations while providing a higher level of linear approximation, which is important for dispersion, shoaling, and orbital velocities.

Similarly to the process for $N=2$, it is possible in higher orders to reduce the number of weighted momentum equations that must be solved simultaneously by eliminating $\mathbf{u}_{N-1,t}$ and $\mathbf{u}_{N,t}$ from weighted

momentum equations $m=(0, N-2)$ through partial Gaussian elimination using momentum equations $m=(N-1, N)$. The remaining $N-1$ equations may be solved for $\mathbf{u}_{0,t}$ to $\mathbf{u}_{N-2,t}$, and the results may then be used to solve for $\mathbf{u}_{N-1,t}$ and $\mathbf{u}_{N,t}$ using momentum equations $m=(N-1, N)$. Again, this is possible because mixed space-time derivatives do not appear in the weighted momentum equations for $n=[N-1, N]$. We will not give details, but the process is very similar to that in Eq. (3.6), except that new coefficients must be found for each equation in $m=(0, N-2)$.

4. Linear properties to very high order

Although nonlinear equations for arbitrary order are long and difficult to write explicitly, it is straightforward to examine linear properties to high order and how they may vary with different choices of basis functions, $f_n(q)$. Both linear dispersion and shoaling are found from the first two orders of a multiple scales expansion, with the linear dispersion found at first order and the shoaling properties at second order. These follow standard, but long, procedures which are detailed in Appendix A.

4.1. Dispersion and orbital velocities

4.1.1. Dispersion

For a given set of basis functions $f_n(q)$, which define integrals g_n , etc., dispersion with changing wavenumber is the most basic linear property. The relationship of orbital velocities to surface elevation also appears as part of the solution for dispersion, and both may be compared to well-known linear hyperbolic solutions (e.g., Dean and Dalrymple, 1991). For a given order of approximation, say $O(\mu^N)$, all valid choices for $f_n(q)$ will yield asymptotic behavior that is also accurate to $O(\mu^N)$ but, like Boussinesq theory, these may be rearranged into forms that are formally more accurate asymptotically, or have other properties that are more useful such as behavior at high wavenumbers. As complexity increases strongly with increasing order, examining general asymptotic rearrangements is simple for $O(\mu^2)$, difficult for $O(\mu^4)$, and a practical impossibility at higher order. However, we may still examine properties at high order for specific sets of basis functions. For comparison, we will use two specific sets of basis functions: simple monomials $f_n \equiv q^n$, and shifted Legendre basis functions $f_n \equiv P_n^*(q)$. The use of monomials is obvious, while shifted Legendre basis functions are orthogonal over the range $q=[0,1]$, and this orthogonality means that many integrals are simplified or zero (Abramowitz and Stegun, 1964). An explicit generation equation is

$$P_n^*(q) = (-1)^n \sum_{k=0}^n q^k \frac{n!}{k!(n-k)!} \frac{(n+k)!}{k!n!} (-1)^k \quad (4.1)$$

Fig. 1 shows linear dispersion for orders of approximation $O(\mu^2, \mu^4, \mu^6, \mu^8)$ for both monomial and shifted Legendre basis functions. When compared to exact linear dispersion of $C_{2t}^2 = \omega^2/k^2 = g \tanh(kh)/kh$, a clear increase in accuracy is seen for both sets of basis functions with increasing level of approximation. For shifted Legendre basis functions, phase speeds have several percent error by $kh=1.5$ at $O(\mu^2)$, while $O(\mu^4)$ remains good until at least $kh=6$. By $O(\mu^6)$, accuracy extends to $kh=15$, while the highest level of approximation, $O(\mu^8)$, has accuracy extending past $kh=20$. Since the nominal deep water limit for water waves is $kh=\pi$, these higher levels of approximation are very accurate.

These may be compared to dispersion results for the simplest possible basis functions, $f_n \equiv q^n$. For the lowest $O(\mu^2)$ solution, accuracy between P_n and q^n dispersion is comparable, but for all higher orders of approximation q^n basis functions give much less accurate results. Because we also expect equations using q^n basis functions to have

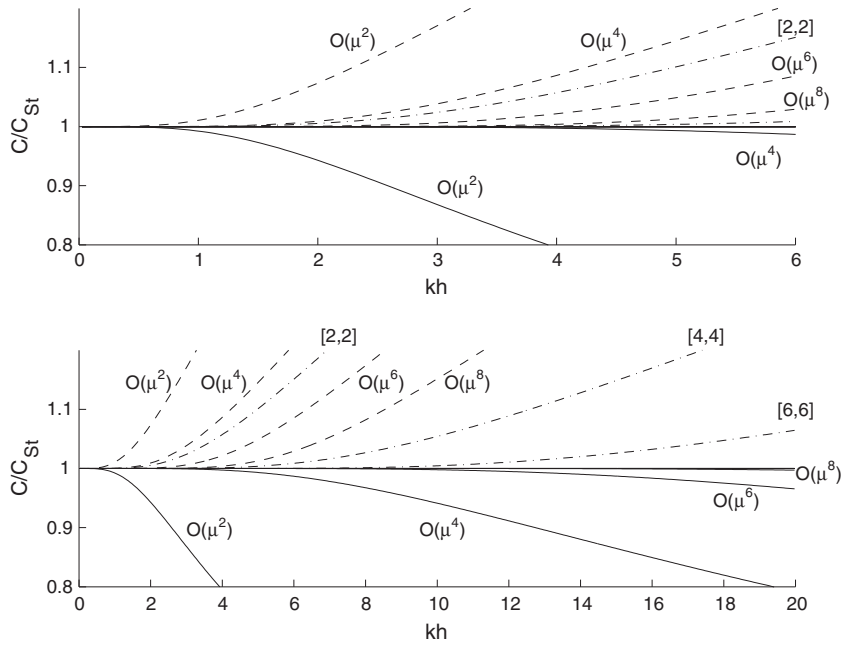


Fig. 1. Approximate dispersion relationships compared to linear Stokes dispersion shown for two different ranges of kh . $O(\mu^2, \mu^4, \mu^6, \mu^8)$. (—) Shifted Legendre basis functions; (---) Monomial basis functions. Padé [2,2], [4,4], and [6,6] dispersion are also shown.

problems with numerical conditioning, we will thus disregard them and use P_n^* as default basis hereinafter.

With the aid of the symbolic manipulation software package Maple, analytical representations may be found for phase speeds. At $O(\mu^2)$, the phase speed using shifted Legendre basis functions is

$$\frac{C^2}{gh} = \frac{1}{1 + \frac{1}{3}(kh)^2} \quad (4.2)$$

which is accurate to $O((kh)^2)$, and is the same as is found for Peregrine's depth-averaged Boussinesq equations, and for Green–Naghdi level I theory (Shields and Webster, 1988). At $O(\mu^4)$ using shifted Legendre basis functions, dispersion becomes

$$\frac{C^2}{gh} = \frac{1 + \frac{13}{105}(kh)^2 + \frac{1}{420}(kh)^4}{1 + \frac{16}{35}(kh)^2 + \frac{3}{140}(kh)^4 + \frac{1}{6300}(kh)^6} \quad (4.3)$$

which is identical to Green–Naghdi theory III (Shields and Webster, 1988) and is accurate to $O((kh)^6)$, which is more accurate than the underlying $O(\mu^4)$ expansion.

For the shifted Legendre polynomial basis functions, the dispersion relation at $O(\mu^6)$ will be

$$\frac{C^2}{gh} = \frac{1 + \frac{14}{99}(kh)^2 + \frac{373}{83160}(kh)^4 + \frac{1}{22680}(kh)^6 + \frac{1}{7983360}(kh)^8}{1 + \frac{47}{99}(kh)^2 + \frac{163}{5544}(kh)^4 + \frac{16}{31185}(kh)^6 + \frac{67}{23950080}(kh)^8 + \frac{1}{279417600}(kh)^{10}} \quad (4.4)$$

which is asymptotically accurate to $O((kh)^{10})$. The dispersion relation at $O(\mu^8)$ will be

$$\frac{C^2}{gh} = \frac{1 + \frac{28}{99}(kh)^2 + \frac{71}{17820}(kh)^4 + \frac{674}{818175}(kh)^6 + \frac{281}{168484800}(kh)^8 + \frac{61}{5507988000}(kh)^{10} + \frac{1}{111307980000}(kh)^{12}}{1 + \frac{47}{99}(kh)^2 + \frac{163}{5544}(kh)^4 + \frac{16}{31185}(kh)^6 + \frac{67}{23950080}(kh)^8 + \frac{1}{279417600}(kh)^{10} + \frac{1}{7912407984000}(kh)^{12}} \quad (4.5)$$

which is asymptotically accurate to $O((kh)^{14})$.

Thus it becomes clear that using the shifted Legendre polynomials provides dispersion accuracy to $O((kh)^{2N-2})$. For all levels greater than $O(\mu^2)$, this is a formal increase in accuracy beyond the nominal order of approximation, and results from the excellent orthogonality

of the polynomials. In contrast, simple monomials only provide accuracy in dispersion to $O((kh)^N)$, which explains the great difference seen in Fig. 1.

4.1.2. Dispersion with generalized basis functions

For lower order systems, it is possible to arrive at dispersion results for generalized basis functions. If we define the most general polynomial system that satisfies Boussinesq scaling, but making sure that the coefficient of highest degree for each basis function is one (which does not imply loss of generality as properties are invariant with respect to a multiplicative constant),

$$\begin{aligned} f_0 &= 1 \\ f_1 &= a + q \\ f_2 &= b + cq + q^2 \\ f_3 &= d + eq + fq^2 + q^3 \\ f_4 &= g + hq + iq^2 + jq^3 + q^4 \end{aligned} \quad (4.6)$$

then the general dispersion relation for an $O(\mu^2)$ system with any choice of (a,b,c) will be

$$\frac{C^2}{gh} = \frac{1 + (\frac{1}{3} + \frac{1}{2}(b-ac))(kh)^2}{1 + (\frac{1}{2} + \frac{1}{2}(b-ac))(kh)^2} \quad (4.7)$$

Thus, although there appear to be three free coefficients, only one combination has any influence on dispersion at $O(\mu^2)$. For the shifted Legendre polynomial basis functions (suitably normalized so that the coefficient of the highest degree polynomial in each basis function is unity), we find $b-ac = -1/3$, while to arrive at the Padé [2,2] approximant as seen in Fig. 1 (Madsen et al., 1991)

$$\frac{C^2}{gh} = \frac{1 + \frac{1}{15}(kh)^2}{1 + \frac{2}{5}(kh)^2} \quad (4.8)$$

we set $b-ac = -1/5$. For the simple monomial basis functions $f_n = q^n$, we find that $b-ac = 0$ which does not yield accurate dispersion.

Although the choice of $b-ac$ still leaves ambiguity in the choice of optimal basis functions, shoaling analyses will help to resolve choices of additional coefficients.

Similarly, we can get the general dispersion relation for an $O(\mu^4)$ system. Instead of having one free parameter, it will vary based on four independent parameters:

$$\begin{aligned} G_1 &= fj - i - 2e \\ G_2 &= fh - ei + 3(dj - g) \\ G_3 &= e \left(g + \frac{i}{3} + \frac{j}{4} + \frac{1}{5} \right) - h \left(d + \frac{f}{3} + \frac{1}{4} \right) \\ G_4 &= e(g + i + j + 1) - h(d + f + 1) \end{aligned} \quad (4.9)$$

The general dispersion relation will then be

$$\frac{C^2}{gh} = \frac{1 + A_1(kh)^2 + A_2(kh)^4 + A_3(kh)^6}{1 + A_4(kh)^2 + A_5(kh)^4 + A_6(kh)^6} \quad (4.10)$$

where

$$\begin{aligned} A_1 &= \frac{1}{6} - \frac{G_1}{12} \\ A_2 &= \frac{1}{120} - \frac{G_1 + G_2}{72} \\ A_3 &= \frac{G_3}{144} \\ A_4 &= \frac{1}{2} - \frac{G_1}{12} \\ A_5 &= \frac{1}{24} - \frac{G_1}{24} - \frac{G_2}{72} \\ A_6 &= \frac{G_4}{144} \end{aligned} \quad (4.11)$$

Note that (a, b, c) do not appear in the system. The four free parameters $G_1 - G_4$ may then be manipulated to improve dispersion properties. To achieve the Padé [4,4] approximant of

$$\frac{1 + \frac{1}{9}(kh)^2 + \frac{1}{945}(kh)^4}{1 + \frac{4}{9}(kh)^2 + \frac{1}{63}(kh)^4} \quad (4.12)$$

which is accurate to $O(kh^8)$, we set $G_1 = 2/3, G_2 = -1/7, G_3 = 0, G_4 = 0$. In order to arrive at the Padé [6,6] approximant (which is accurate to $O((kh)^{12})$):

$$\frac{C^2}{gh} = \frac{1 + \frac{5}{39}(kh)^2 + \frac{2}{715}(kh)^4 + \frac{1}{135135}(kh)^6}{1 + \frac{6}{13}(kh)^2 + \frac{10}{429}(kh)^4 + \frac{4}{19305}(kh)^6} \quad (4.13)$$

we choose $G_1 = 6/13, G_2 = -9/143, G_3 = 16/15015, G_4 = 64/2145$. Thus, there are many basis functions that could give other relations within the context of Eq. (4.10) as desired. Both of the Padé approximants at $O(\mu^4)$ provide significantly improved dispersion when compared to the Shifted Legendre polynomials, with accuracy potentially increasing from $kh = 6$ to $kh > 10$. These should also improve significantly short wavelength results.

It should be noted that both the $O(\mu^2)$ equations with Padé [2,2] dispersion and the $O(\mu^4)$ equations with Padé [6,6] dispersion still have free coefficients which may be used to simultaneously optimize dispersion and shoaling in the next section. Higher order μ^6 and μ^8 equations will also have free coefficients that may be used to optimize properties, but the systems become extremely complex. Additionally, the accuracy from using shifted Legendre polynomials is so great at these levels that additional manipulation seems unnecessary.

4.1.3. Orbital velocities

In addition to wave speeds, orbital velocities can be extremely important. Figs. 2–3 show magnitudes of horizontal and vertical

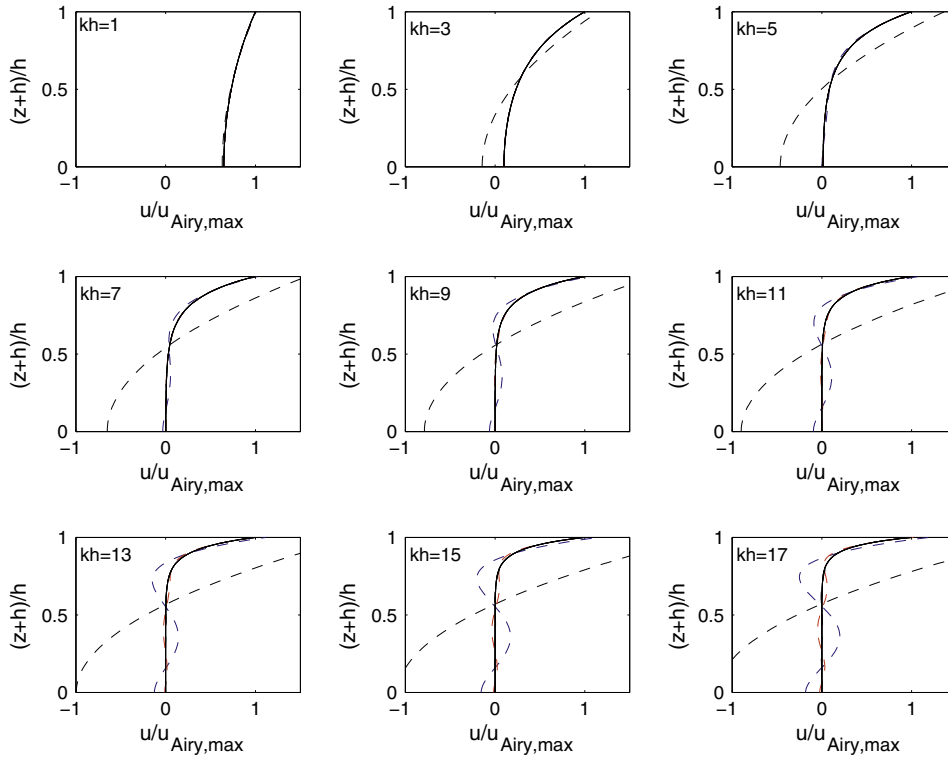


Fig. 2. Horizontal orbital velocities for wavenumbers from shallow to very deep water using shifted Legendre basis functions. Solid line is exact linear Stokes solution; (black dashed) $O(\mu^2)$; (blue dashed) $O(\mu^4)$; (red dashed) $O(\mu^6)$; (almost indistinguishable from exact solution) $O(\mu^8)$. (For interpretation of the references to color in this figure legend, the reader is referred to the web version of this article.)

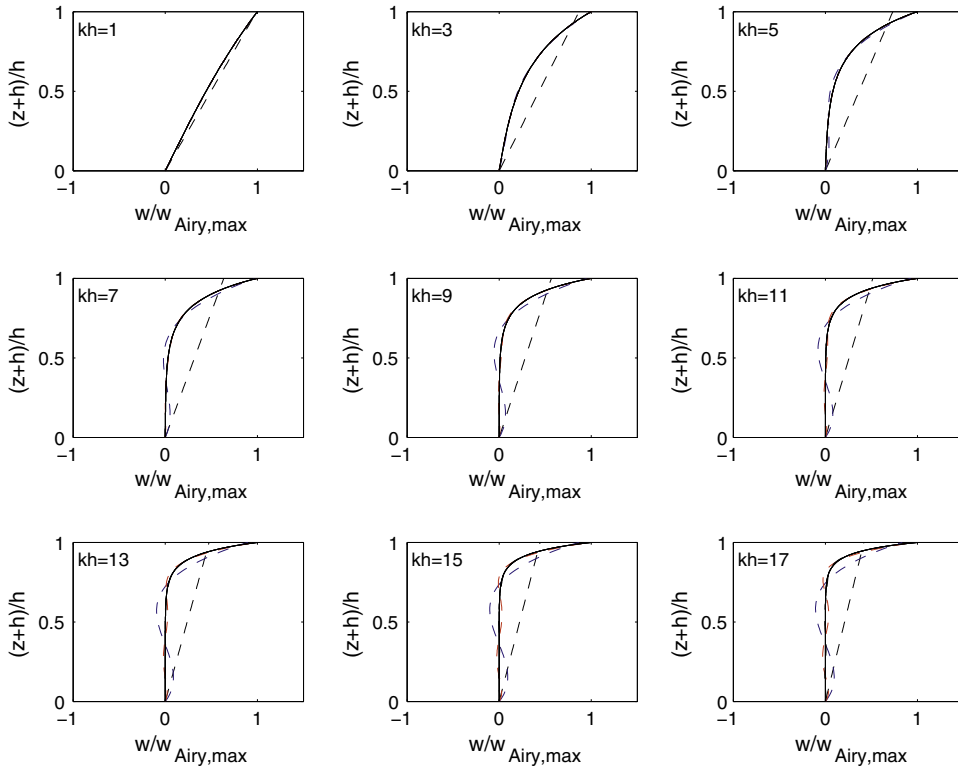


Fig. 3. Vertical orbital velocities for wavenumbers from shallow to very deep water using shifted Legendre basis functions. Solid line is exact linear Stokes solution; (black dashed) $O(\mu^2)$; (blue dashed) $O(\mu^4)$; (red dashed) $O(\mu^6)$; (almost indistinguishable from exact solution) $O(\mu^8)$. (For interpretation of the references to color in this figure legend, the reader is referred to the web version of this article.)

velocities for shifted Legendre basis functions compared to exact solutions (Dean and Dalrymple, 1991). All levels of approximation show good results for small wavenumbers $kh=1$, with $O(\mu^2)$ relations losing accuracy by $kh=3$, $O(\mu^4)$ results beginning to lose

accuracy by $kh=7$, $O(\mu^6)$ systems beginning to lose accuracy by $kh=15$, and $O(\mu^8)$ velocities showing good agreement with exact results all the way up to $kh=17$. Again, these are quite good and in line with dispersion relations. Importantly, both horizontal and

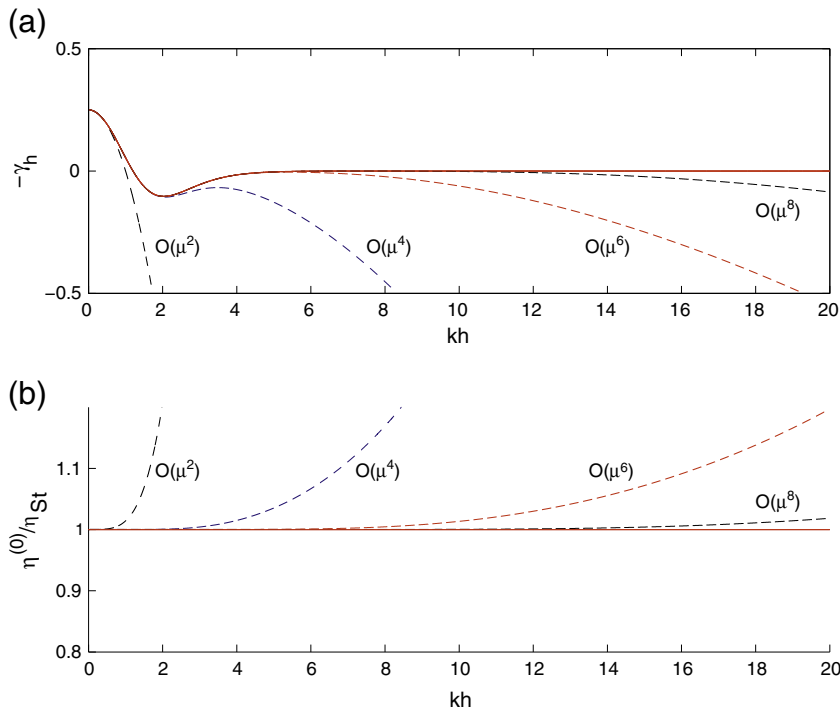


Fig. 4. (a) Shoaling gradients; and (b) Integrated shoaling amplitudes from shallow to deep water compared to linear Stokes theory for varying dimensionless wavenumbers and using shifted Legendre basis functions. $O(\mu^2, \mu^4, \mu^6, \mu^8)$. (red) Exact solutions. (For interpretation of the references to color in this figure legend, the reader is referred to the web version of this article.)

vertical orbital velocities show convergence with increasing order of approximation, unlike straightforward Boussinesq expansions that diverge for moderate wavenumbers (Kennedy and Kirby, 2002; Madsen and Agnon, 2003). This convergence provides further evidence of the utility for this method and provides increased confidence in internal velocities once turbulent/viscous stresses are added to the model.

However velocities are not perfect, and inspection of Fig. 2 shows that the horizontal bottom velocity, which is of utmost importance for sediment transport and determination of frictional stresses, actually shows the wrong sign for very high wavenumbers, and is opposite the direction of the surface velocity. This gives another measure of the accuracy limits for each order of approximation, and the changeover wavenumbers from positive to negative bottom velocity comes at $kh = (2.45, 5.09, 7.73, 10.38)$ for $O(\mu^2, \mu^4, \mu^6, \mu^8)$, respectively. In comparison, the changeover wavenumber for Nwogu's (1993) $O(\mu^2)$ Boussinesq equations with $z_\alpha = -0.553h$ (resulting in Padé [2,2] dispersion), is $kh = \sqrt{10} \approx 3.16$.

4.2. Shoaling

Fig. 4a compares approximate and exact shoaling gradients for shifted Legendre basis functions for $O(\mu^2, \mu^4, \mu^6, \mu^8)$. These follow a very similar progression to the linear dispersion relations of Fig. 1, as might be expected. Higher order μ^8 shoaling is again extremely accurate up to very high wavenumbers with lower order systems decreasing in accuracy. It should be noted that all errors in shoaling gradient are negative – i.e., any cumulative shoaling errors for a wave traveling from deep to shallow water would tend to make it too small rather than too large. This is preferred for numerical and stability reasons. This cumulative shoaling error may be quantified by integrating the shoaling gradient from deep to shallow water as in Chen and Liu (1995) to get

$$\frac{\eta^{(0)}}{\eta_{St}} = \exp \left[\int_0^{kh} \frac{\gamma_h(kh') - \gamma_B(kh')}{(kh')} d(kh') \right] \tag{4.14}$$

where γ_B is the approximate shoaling gradient. This is shown in Fig. 4b, and demonstrates a similar range of applicability, with $O(\mu^2)$ equations losing accuracy by $kh \approx 2$, while $O(\mu^8)$ equations are again showing only a few percent error by $kh = 20$.

4.2.1. Shoaling with optimized coefficients

Shoaling gradients may also be optimized using generalized basis functions. For $O(\mu^2)$ equations, and using $b - ac = -1/5$ to achieve Padé [2,2] dispersion, the associated shoaling relation is

$$\gamma_h = -1/4 \frac{(84 + 200a)(kh)^8 + (490 + 1000a)(kh)^6 + (3150 + 7500a)(kh)^4 - 4125(kh)^2 + 5625}{(75 + 10(kh)^2 + 2(kh)^4)^2} \tag{4.15}$$

Its Taylor series expansion will be:

$$\gamma_h = -1/4 + 1/4(kh)^2 + \left(-\frac{17}{90} - 1/3 a\right)(kh)^4 + O(\mu^6) \tag{4.16}$$

To match the Taylor expansion of the exact solution at $O(\mu^4)$,

$$\gamma_h = -1/4 + 1/4(kh)^2 - 1/18(kh)^4 + O(\mu^6) \tag{4.17}$$

$a = -2/5$. This is shown in Fig. 5 and compared to the exact linear solution.

However, matching Taylor series coefficients is not the only way to optimize shoaling. By setting $a = -21/50$, shoaling gradients may be matched for infinite depths: that is to say, the deep water shoaling gradient will be identically zero. This gives slightly higher error at lower wavenumbers, but the integrated error remains relatively small even in extremely deep water. A third optimization method is to minimize the squared error between exact shoaling and approximate amplitudes over a range, say $kh = [0,4]$. This results in $a = -0.432$, which is seen in Fig. 5 to give good agreement over the useful range of the approximation.

We have still not set the precise basis functions as we only have two constraints, but three free coefficients, a, b, c . Indeed, no third

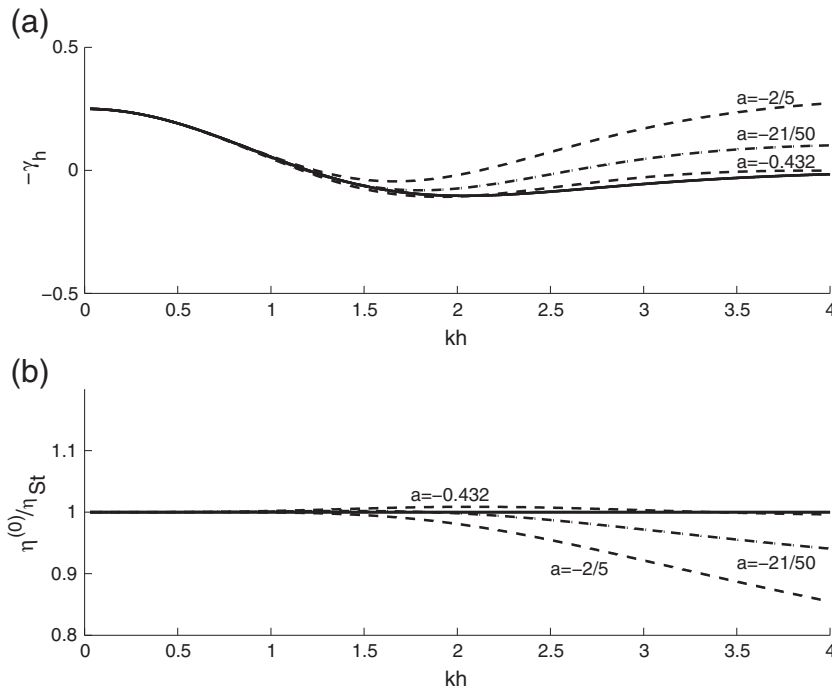


Fig. 5. (a) Shoaling gradients; and (b) Integrated shoaling amplitudes from shallow to deep water compared to linear Stokes theory for varying dimensionless wavenumbers, $O(\mu^2)$. (solid line) Exact solutions; (Long Dash) Taylor series match with $a = -2/5$; (Dash-Dot) Infinite depth match with $a = -21/50$; (Dotted) Least-squares optimization between $kh = [0,4]$ with $a = -0.432$.

constraint appears possible as because any set of linear combinations of basis functions can be made with only two constraints by adding multiples of function f_1 to f_2 . Because of this, any set of a, b, c at $O(\mu^2)$ satisfying the two constraints should yield identical properties overall, not just for linear dispersion and shoaling. For these reasons, we arbitrarily set $c=0$, which then fixes a and b . Values for coefficients in the optimized basis functions are given in Table 2 for Padé [2,2] dispersion and all shoaling optimizations.

As can be expected, optimization of shoaling becomes much more complex for higher order equations. Here, we have not attempted a completely general shoaling analysis at $O(\mu^4)$, as this quickly became too complex. Instead, we perform shoaling optimization for Padé [6,6] dispersion, which is the most accurate possible for these $O(\mu^4)$ equations. As shown in Section 4.1.2, this requires four constraints on parameters G_1 to G_4 , leaving additional degrees of freedom.

Once dispersion constraints are specified, only two new combinations of variables affect shoaling performance: $G_5 = e$, and $G_6 = ej - h$. As with the $O(\mu^2)$ equations, we offer two possibilities for shoaling optimization: (i) equating as many terms in the Taylor series of (A.16) using free coefficients $G_5 - G_6$; and (ii) minimizing integrated error compared using Eq. (4.14) over the range $kh = [0, 10]$.

As seen in Fig. 6, shoaling performance becomes considerably improved with the Padé [6,6] dispersion and shoaling constraints when compared to shifted Legendre basis functions. While the $O(\mu^4)$ shifted Legendre performance is already accurate to the deep water limit of $kh = \pi$, the Taylor series match to $O(\mu^8)$ improves agreement until $kh = 6$, which nearly doubles its region of accuracy. Optimizing the shoaling coefficients over the range $kh = [0, 10]$ increases error slightly for lower wavenumbers but allows for shoaling with maximum possible errors of only a few percent all the way to $kh = 20$, which is excellent. Thus, the optimization can give good dispersion and shoaling performance for $O(\mu^4)$ systems well beyond the depth range where these models are likely to be used.

These optimizations still do not specify uniquely the $O(\mu^4)$ basis function coefficients. To do this, we will wait until the next section, when nonlinear properties may be used to further optimize performance and produce additional constraints.

5. Nonlinear properties

Nonlinear properties provide an additional test of accuracy for these systems, and are potentially another source of basis function optimization. Second harmonics for a steady wave are the most basic test, and tend to give the trend for properties at higher order. These may be examined using standard nonlinear expansions (Kennedy et al., 2001; Madsen and Schäffer, 1998; Nwogu, 1993), where $\eta = \eta^{(0)} + \eta^{(1)} + \dots$, where η is a nonlinear amplitude expansion parameter. At lowest order, this expansion provides linear dispersion as in the previous sections and gives the relationship between surface elevations and velocities. The second order equations, however, are different from the shoaling analysis, and will give

Table 2
Recommended basis function coefficients for optimized dispersion and shoaling.

| Coefficient | $O(\mu^2)$ with Padé [2,2] dispersion, Low shoaling error, $kh = [0, 4]$ | $O(\mu^4)$ with Padé [6,6] dispersion, Low shoaling error, second harmonic error, $kh = [0, 10]$ |
|-------------|--|--|
| a | -0.432 | -0.03 |
| b | -1/5 | 0.135 |
| c | 0 | 0 |
| d | | -0.07332106862 |
| e | | 0.72 |
| f | | -1.607627232 |
| g | | -0.1314065934 |
| h | | 1.136 |
| i | | -1.901538462 |
| j | | 0 |

second surface harmonics and modifications to orbital velocities. Second harmonics may be compared with exact second order Stokes wave harmonics (e.g. Dean and Dalrymple, 1991). Because nonlinear equations of arbitrary order are outside the scope of this paper, we only include nonlinear terms up to $O(\mu^2)$. We will consider levels of dispersion $O(\mu^2)$ and $O(\mu^4)$. These give four systems of equations which may also be optimized using different basis functions if desired. Details of the expansion techniques are again standard, and are given in Appendix B.

At $O(\mu^4)$ and higher when using $O(\mu^2)$ nonlinearity, the possibility exists for further optimization of nonlinear harmonics. Here, the coefficient groups $b-ac$ and a appear in second order equations even though they have no influence on linear properties at $O(\mu^4)$ or higher. These coefficients may be used to improve the performance of second order harmonics, either by matching Taylor series coefficients, or by optimizing performance over a range. As with shoaling, we have taken two approaches to this optimization: the two free coefficients were used either to (i) equate the next two terms in the Taylor series of second harmonics to the exact Stokes values; or (ii) manipulate coefficients to produce small errors over a specified range. Because of the great complexity of the dispersion, shoaling and second order nonlinear equations for high order equations, this nonlinear optimization was only performed at $O(\mu^4)$. Multiple sets of coefficients were found for Taylor series matches arising from the multiple roots in quadratic and higher order equations. Despite having the same Taylor series matches, these different roots could give quite different properties.

Fig. 7 shows second harmonics compared to exact Stokes solutions (Dean and Dalrymple, 1991) for numerous basis functions at $O(\mu^2)$ and $O(\mu^4)$. While shifted Legendre basis functions at $O(\mu^2)$ show a monotonic decrease in nonlinearity when compared to exact solutions and have errors in the second harmonic that are asymptotically $O(\mu^2)$, optimized dispersion gives much more accurate nonlinearity with errors that are asymptotically $O(\mu^4)$, has total errors of less than 20% for $kh < 1.7$, and is accurate to within 36% for the range $0 < kh < 6$. Furthermore, errors over this range tend to give weaker nonlinearity, which is extremely helpful for numerical implementation. It should be noted that second order superharmonic behavior for the optimized $O(\mu^2)$ dispersion including $O(\mu^2)$ nonlinearity is identical to the 'datum invariant' equations of Kennedy et al. (2001) optimized for Padé [2,2] dispersion, even though the systems were derived through very different methods. These previous 'datum invariant' equations are generalizations of the Wei et al. (1995) equations so that the reference elevation is defined at a constant fraction of the instantaneous water depth, which is equivalent to a fixed sigma coordinate. In this way, the connection to the present system may be seen.

At $O(\mu^4)$ dispersion using shifted Legendre basis functions, nonlinear behavior shows little improvement when compared to $O(\mu^2)$, despite the great improvement in linear dispersive accuracy; this because only $O(\mu^2)$ nonlinear terms were retained in the new systems for reasons of complexity. However, dispersion, shoaling, and second order nonlinear optimization through asymptotic rearrangement can significantly improve all parameters. Many different optimizations were tried but some, for example, might improve asymptotic properties very well at low wavenumbers but have pathological performance for high wavenumbers. Fig. 7 shows second harmonics for several optimizations at $O(\mu^4)$. The first has Padé [6,6] dispersion, $(kh)^8$ accurate shoaling, and $(kh)^6$ second harmonics. Here, good agreement is found at low wavenumbers but relative error in the second harmonic increases greatly for both root as wavenumbers increase, making the coefficient sets largely unusable.

The second optimization also uses Padé [6,6] dispersion as in Section 4.1.2, optimizes shoaling over the range $kh = [0, 10]$ as in Section 4.2.1, and uses the remaining free coefficients to optimize the second harmonic over the same range. This gives slightly larger

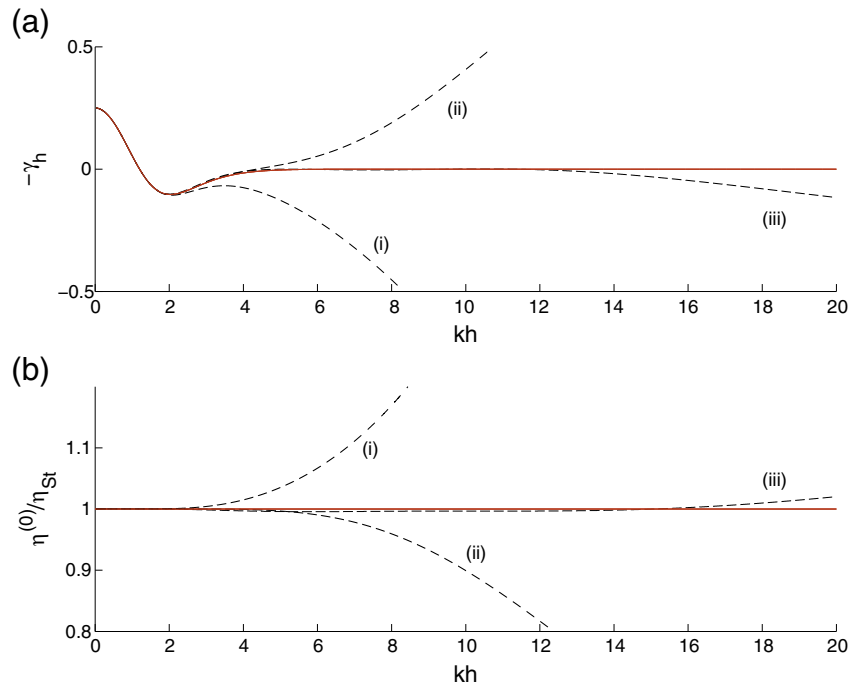


Fig. 6. (a) Shoaling gradients; and (b) Integrated shoaling amplitudes from shallow to deep water compared to linear Stokes theory for varying dimensionless wavenumbers, $O(\mu^4)$. (solid line) Exact solutions; (i) Shifted Legendre basis functions; (ii) Padé [6,6] dispersion, $(kh)^8$ Taylor series shoaling; (iii) Padé [6,6] dispersion, optimized shoaling coefficients over range $kh = [0,10]$.

error for lower wavenumbers but has a maximum error of less than 4% over the range shown. Both of these are clear improvements over the shifted Legendre basis functions, and again demonstrate the power of asymptotic rearrangements.

Linear dispersion, shoaling, and nonlinear constraints may now be used to define basis function coefficients. There are still remaining degrees of freedom that arise from the possibility of linear combinations of basis functions, and do not appear to influence properties. Thus, we arbitrarily set $c = 0$ and $j = 0$ to provide the final constraints and solve

for the basis function coefficients for the different optimizations. Because of the greater complexity of higher order systems, it was only possible to obtain numerical values for coefficients rather than the exact solutions found for $O(\mu^2)$. These coefficients define basis functions and corresponding evolution equations, that may then be used in more general conditions as shown in the next section. It is clear from Fig. 7 that many of the coefficient sets will have poor nonlinear behavior at high wavenumbers; thus Table 2 gives detailed coefficients only for set (iii) of Fig. 7, with Padé [6,6] dispersion, and shoaling and second

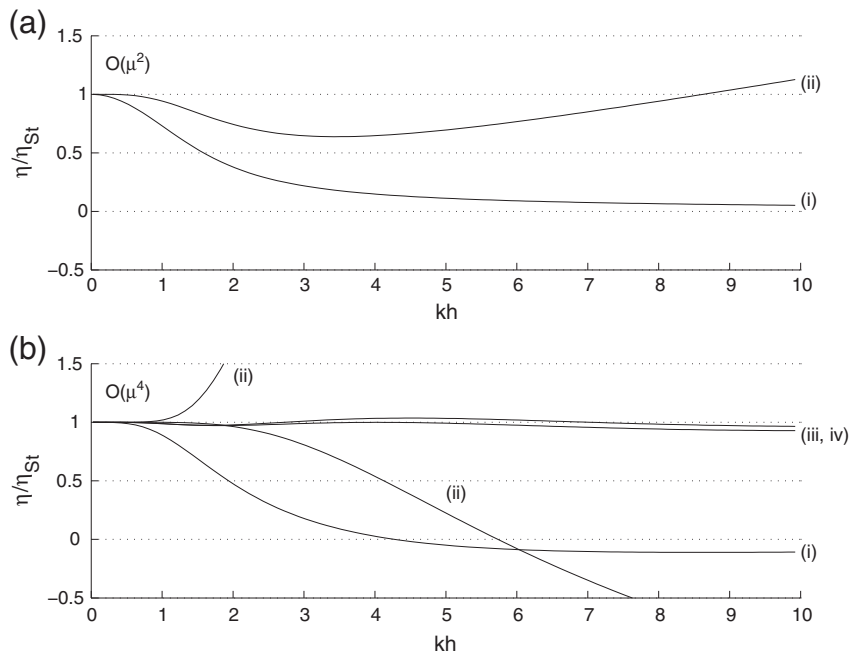


Fig. 7. Model second order harmonic compared to full Stokes solution for steady wave. (a) $O(\mu^2)$ equations: (i) Shifted Legendre basis functions; (ii) Taylor series optimized dispersion and shoaling to $(kh)^4$. (b) $O(\mu^4)$ equations: (i) Shifted Legendre basis functions; (ii) Padé [6,6] dispersion, Taylor series $(kh)^8$ shoaling, $(kh)^6$ second harmonic; (iii) Padé [6,6] dispersion, shoaling and second harmonic errors minimized over $kh = [0,10]$; (iv) Padé [6,6] dispersion, Taylor series $(kh)^8$ shoaling, second harmonic errors minimized over $kh = [0,10]$.

harmonic error optimized over $kh=[0,10]$. This recommended set should give good results for a variety of simulations.

6. Numerical tests: wave transformation over a submerged shoal

The transformation of a wave train passing over a trapezoidal shoal is a standard test in Boussinesq and Green–Naghdi-type wave models as it tests not only linear dispersion and shoaling performance, but also nonlinear shoaling and fissioning. Here, we use the data reported in *Beji and Battjes (1993)* and *Dingemans (1994)*, which has been used for comparison by numerous researchers (*Barthelemy, 2004; Beji and Battjes, 1994; Chazel et al., 2011; Gobbi and Kirby, 1999*). Fig. 8 shows the experimental setup and measurement locations, with stations before, on, and after the bar. All data and computations show largely linear waves before the bar, nonlinear peaked waves on the bar in early stages of fissioning, and complex multifrequency waves after the bar as bound higher harmonics are released in deeper water.

Computations here were performed for both $O(\mu^2)$ and $O(\mu^4)$ equations using a standard central differencing scheme in one horizontal dimension and fourth order Runge–Kutta time differencing. A spatial resolution of $\Delta x=0.025$ m and $\Delta t=0.02$ s was used for all tests shown here. Additional resolutions were also tested and did not show significant differences. Lower order computations used the optimized set with Padé [2,2] dispersion and shoaling optimized over $kh=[0,4]$ in Table 2, while $O(\mu^4)$ computations used the Padé [6,6] dispersion and both shoaling and nonlinear properties optimized over $kh=[0,10]$. The computational boundaries had reflecting walls without sponge layers to absorb waves, but the domain was large enough that reflected waves did not reappear in the areas of interest before the end of the simulations.

Fig. 9 shows time series of measured and computed water surface elevations for Case A with $T_p=2.02$ s and initial wave height $H=2$ cm using the optimized $O(\mu^2)$ equations with Pade [2,2] dispersion. Agreement on the bar is excellent, where the wave has a sharply peaked form and appears to be fissioning like a solitary wave on a shelf. After the bar, the wave releases its bound harmonics which then travel largely as free waves at their own speeds. Agreement remains good here although errors may be seen to accumulate with increasing distance from the bar, as the higher harmonics are not simulated as well by these $O(\mu^2)$ equations. Agreement here is quite similar to other optimized $O(\mu^2)$ equations including the WKGS equations shown in *Gobbi and Kirby (1999)*, the equations of *Madsen et al. (1991)* and *Madsen and Sørensen (1992)* as reported by *Dingemans (1994)*, and Green–Naghdi type solutions (*Chazel et al., 2011*). For this level of approximation, it appears that accuracy is limited by the Pade [2,2] or similar dispersion and any improvement demands a similarly improved dispersion relation.

Fig. 10 shows results for the higher $O(\mu^4)$ equations with Padé [6,6] dispersion, and optimized shoaling and second harmonics over the range $kh=[0,10]$. The other $O(\mu^4)$ coefficients in Table 2 give almost identical results. Before on, and immediately after the shoal,

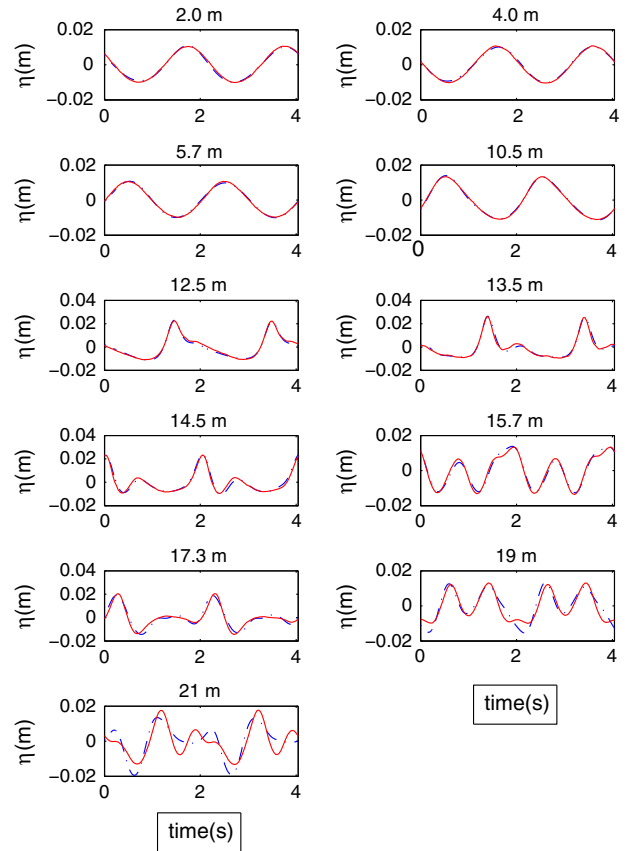


Fig. 9. Computed and measured time series of wave transformation over a submerged shoal, $O(\mu^2)$ equations, Padé [2,2] dispersion, optimized shoaling $kh=[0,4]$.

$O(\mu^4)$ results are almost identical to the $O(\mu^2)$ solution, showing that this gives a good simulation of the actual processes in these regions. However, the improved dispersion of the $O(\mu^4)$ equations becomes apparent by $x=21$ m, when the higher order equations give a much better prediction of the water surface. These results are quite good and are comparable to the weakly nonlinear WN4 simulations of *Gobbi and Kirby (1999)* over the same topography. However, the present $O(\mu^4)$ solutions still have some errors in higher harmonic terms and are not as accurate as *Gobbi and Kirby's* fully nonlinear FN4 equations for this problem. This is because the FN4 equations keep more nonlinear terms than the present models, although at the price of much more complexity. Thus, even though we have optimized dispersion, shoaling and second harmonics, the higher order nonlinear behavior does not appear to be automatically improved, and limits are apparent. Still, accuracy appears to be quite good, and is adequate for almost all nearshore purposes, particularly when we consider that the model may be naturally extended to include rotational processes in the surf zone.

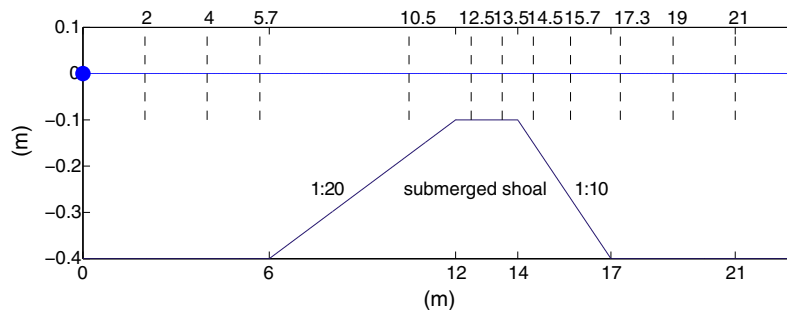


Fig. 8. Experimental setup for wave transformation over a submerged shoal, showing gauge locations.

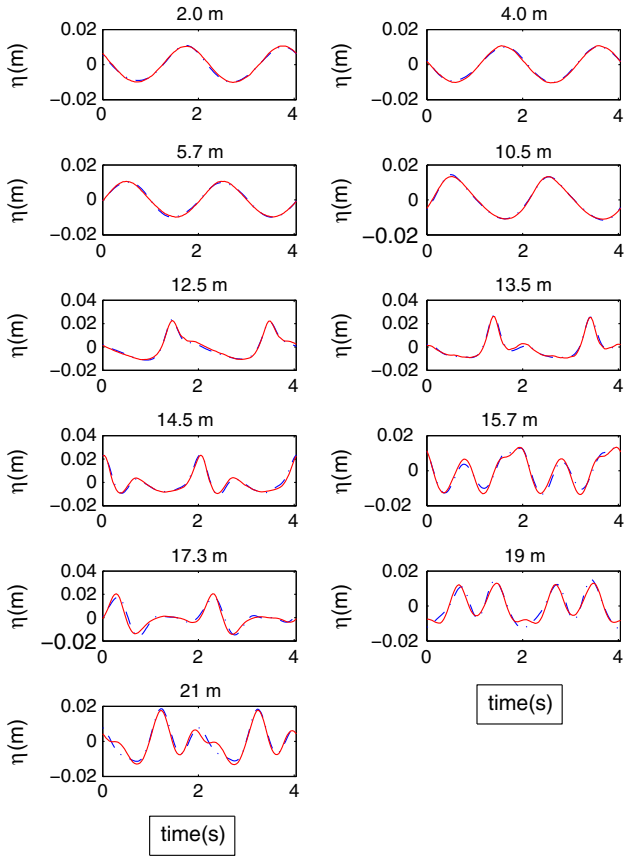


Fig. 10. Computed and measured time series of wave transformation over a submerged shoal, $O(\mu^4)$ equations, Padé [6,6] dispersion, optimized shoaling and second harmonics over $kh = [0, 10]$.

7. Discussion and conclusions

The inclusion of rotationality in the present formulations was not important in the examples here, which were inviscid and irrotational wave problems; still the use of a fundamentally rotational model that mimics existing Boussinesq results both analytically and numerically gives good confidence in its ability outside the surf zone. For extension into the surf zone and through to the shoreline, additional viscous/turbulent stresses need to be specified corresponding to breaking wave dissipation and bottom stresses; these are under development and will be detailed in a future publication. The present formulation has the great advantage that because it is derived without any irrotationality conditions, it will be able to make use of more standard turbulence closures and thus needs to make fewer ad-hoc breaking assumptions than many other Boussinesq-type breaking models (e.g. Kennedy et al., 2000a). It may also prove advantageous in some situations to introduce a second shallow water rotational scaling, which will allow for the representation of bottom boundary layer and similar processes without a large increase in the Boussinesq dispersive order.

The systems of equations derived here have properties that fall directly within the range of standard Boussinesq and Green–Naghdi models, but provide some useful extensions, particularly in that velocity modes are not slaved to each other by irrotationality.

The generalization of velocity basis functions combined with Boussinesq scaling allows for asymptotic rearrangements similar in character to those of Nwogu (1993), Madsen and Schäffer (1998) and others, and with similar improvements in accuracy. For linear properties of $O(\mu^2)$ and higher, generalized analysis using arbitrary

basis functions becomes highly complex but the use of shifted Legendre polynomials, which have excellent orthogonality properties, provides accuracy that is considerably higher than the formal level of approximation for both linear dispersion and shoaling ($O(\mu^{2N-2})$). This is particularly obvious when compared with simple monomial basis functions.

Fully nonlinear systems up to $O(\mu^2)$ are straightforward to derive and code by hand. Linear components up to arbitrary order may also be explicitly written and coded without great difficulty, but the nonlinear components become extremely complex. As such, $O(\mu^2)$ may represent a practical limit to nonlinearity for these types of systems. It is quite possible to develop codes that automatically sum and integrate the nonlinearity without ever writing down the system on paper. However, related developments using many of the same concepts as the present paper, including Boussinesq and rotational shallow water scalings and asymptotic rearrangement, may prove to be better candidates for very high order representation of nonlinearity. In any case, as mentioned in the Introduction, the assumption of a single-valued free surface $\eta(x, y, t)$ will impose an upper limit on surf zone accuracy, particularly in regions of strong plungers.

Still, the systems here represent a significant advance in that they can naturally represent rotational processes while keeping many of the advantages of standard Boussinesq and Green–Naghdi formulations. The demonstrated linear convergence for higher order equations is also significant.

Acknowledgments

This work was funded under the National Science Foundation grant 102519, and by the Office of Naval Research under the award N00014-11-1-0045. Their support is gratefully acknowledged. Digital data files for wave propagation over a shoal were provided by Maarten Dingemans.

A. Multiple scale expansions to obtain linear dispersion and shoaling properties

The multiple scales expansion in space (assuming that the system is purely periodic in time) has fast and slow spatial derivatives x and X_1 , respectively

$$\begin{aligned} u_{n,t} &\rightarrow u_{n,t} \\ u_{n,xt} &\rightarrow u_{n,xt} + \epsilon u_{n,X_1t} u_{n,xt} \rightarrow u_{n,xt} + \epsilon u_{n,XX_1t} + \epsilon u_{n,X_1,xt} + O(\epsilon^2) \end{aligned} \quad (\text{A.1})$$

with similar expressions for η . As is standard, fast derivatives will be of leading order while slow derivatives are of $O(\epsilon)$.

As an example, defining the water depth to be only slowly varying and thus have only slow X_1 derivatives, the horizontal derivative of the linearized pressure equation (Eq. (2.8)), to $O(\epsilon h_{X_1})$, is then

$$\begin{aligned} \frac{\partial P}{\partial X} &= \sum_{n=0}^{N-2} \mu^{\beta_n+2} \left[-u_{n,XX_1t} h^2 (G_n|_{q=1} - G_n) \right] + g \eta_x \\ &+ \epsilon \sum_{n=0}^{N-2} \mu^{\beta_n+2} \left[-\left(u_{n,XX_1t} + u_{n,X_1,xt} \right) h^2 (G_n|_{q=1} - G_n) \right] \\ &+ \epsilon h h_{X_1} \sum_{n=0}^{N-2} \mu^{\beta_n+2} u_{n,xt} \left[-2(G_n|_{q=1} - G_n) + (R_n|_{q=1} - R_n) \right. \\ &\left. - g_n|_{q=1} - g_n q + 2g_n \right] + \epsilon g \eta_{X_1} + O(\mu^{N+2}) \end{aligned} \quad (\text{A.2})$$

while a multiple scales expansion for the mass equation gives

$$\eta_{,t} + \sum_{n=0}^N g_n|_{q=1} \left[\left(u_{n,x} + \epsilon u_{n,X_1} \right) h + \epsilon u_n h_{X_1} \right] = 0 \quad (\text{A.3})$$

Now expand each component in a perturbation series: $\eta = \eta^{(0)} + \eta^{(1)}$, $u_n = u_n^{(0)} + u_n^{(1)}$. Insert these into Eqs. (3.7) and (3.8), and collect all terms into the various orders to get perturbation equations: At $O(1)$

$$\begin{aligned} \eta_{,t}^{(0)} + \sum_{n=0}^N g_n |_{q=1} u_{n,x}^{(0)} &= 0 \\ h \left(\sum_{n=0}^N \phi_{mn} |_{q=1} u_{n,t}^{(0)} - \sum_{n=0}^{N-2} u_{n,xt}^{(0)} h^2 (g_m |_{q=1} G_n |_{q=1} - \Gamma_{mn} |_{q=1}) \right. \\ &\left. + g_m |_{q=1} (g \eta_{,x}^{(0)}) \right) = 0, m = [0, N] \end{aligned} \quad (\text{A.4})$$

At $O(\epsilon)$,

$$\begin{aligned} \eta_{,t}^{(1)} + \sum_{n=0}^N g_n |_{q=1} u_{n,x}^{(1)} &= -a^{(1)} \\ h \left(\sum_{n=0}^N \phi_{mn} |_{q=1} u_{n,t}^{(1)} - \sum_{n=0}^{N-2} u_{n,xt}^{(1)} h^2 (g_m |_{q=1} G_n |_{q=1} - \Gamma_{mn} |_{q=1}) \right. \\ &\left. + g_m |_{q=1} (g \eta_{,x}^{(1)}) \right) = -b_m^{(1)}, \end{aligned} \quad (\text{A.5})$$

where $m = [0, N]$,

$$a^{(1)} = \sum_{n=0}^N g_n |_{q=1} (u_{n,x_1}^{(0)} h + u_n^{(0)} h_{,x_1}) \quad (\text{A.6})$$

$$\begin{aligned} b_m^{(1)} &= h \sum_{n=0}^{N-2} - (u_{n,x_1,t}^{(0)} + u_{n,xx_1,t}^{(0)}) h^2 (g_m |_{q=1} G_n |_{q=1} - \Gamma_{mn} |_{q=1}) \\ &+ h^2 h_{,x_1} \sum_{n=0}^{N-2} u_{n,xt}^{(0)} [-2 (g_m |_{q=1} G_n |_{q=1} - \Gamma_{mn} |_{q=1}) \\ &+ (g_m |_{q=1} R_n |_{q=1} - \Theta_{mn} |_{q=1}) - g_m |_{q=1} g_n |_{q=1} \\ &+ 2\gamma_{mn} |_{q=1} - \theta_{mn} |_{q=1}] + h g_m |_{q=1} (g \eta_{,x_1}^{(0)}), m = [0, N] \end{aligned} \quad (\text{A.7})$$

Taking each component (at any order)

$$\eta \equiv \tilde{\eta} e^{i\psi} + c.c. \quad u_n \equiv \tilde{u}_n e^{i\psi} + c.c. \quad (\text{A.8})$$

where $\psi_{,x} \equiv k(X_1)$, $\psi_{,t} \equiv -\sigma$, and c.c. refers to the complex conjugate. We then substitute into Eqs. (A.4)–(A.7) and solve.

At first order, the system is closed and the linear dispersion relations may be found by setting the determinant of Eq. (A.4) to zero. At second order, the system is still not closed because there are more unknowns than equations, and more constraints must be developed. First, we specify $\tilde{\eta}_0^{(2)} = 0$, so that the wave height on the slope is the same as on a flat bed. Next we relate k_{X_1} to $h_{,X_1}$. If we write the dispersion relation as $\sigma^2/gk = Q(kh)$ then

$$k_{,X_1} = -h_{,X_1} \frac{k}{h} \frac{khQ_{,kh}}{Q + khQ_{,kh}} = h_{,X_1} k_{tr} \quad (\text{A.9})$$

$$(kh)_{,X_1} = h_{,X_1} k \left(1 - \frac{khQ_{,kh}}{Q + khQ_{,kh}} \right) = h_{,X_1} [kh]_{tr} \quad (\text{A.10})$$

where the derivative of Q is with respect to kh . This works for all dispersion relations, when the appropriate expressions are used for approximate or exact quantities.

Finally, we must relate $\tilde{u}_{n,X_1}^{(0)}$ to $\tilde{\eta}_{,X_1}^{(0)}$ through the dispersion matrix. All of these relationships will have the form

$$\frac{\tilde{u}_n^{(0)}}{\sigma \tilde{\eta}^{(0)}} = T_n(kh) \quad (\text{A.11})$$

This leads to

$$\begin{aligned} \tilde{u}_{n,X_1}^{(0)} &= \tilde{\eta}_{,X_1}^{(0)} \sigma T_n + \tilde{\eta}^{(0)} \sigma T_{n,kh} [kh_{,X_1} + k_{,X_1} h] \\ &= \tilde{\eta}_{,X_1}^{(0)} \sigma T_n + \tilde{\eta}^{(0)} \sigma T_{n,kh} h_{,X_1} [kh]_{tr} \end{aligned} \quad (\text{A.12})$$

which, once it is noted that $\tilde{\eta}_{,X_1}^{(0)} = \tilde{\eta}_{,h}^{(0)} h_{,X_1}$, closes the system.

The revised equations are then

$$\begin{aligned} a^{(1)} &= h_{,X_1} \sum_{n=0}^N g_n |_{q=1} (\tilde{\eta}_{,h}^{(0)} h \sigma T_n + \tilde{\eta}^{(0)} (\sigma T_n + h \sigma T_{n,(kh)} [kh]_{tr})) \\ b_m^{(1)} &= +h h_{,X_1} \sum_{n=0}^{N-2} -\sigma^2 k T_n \tilde{\eta}^{(0)} h^2 (2g_m |_{q=1} G_n |_{q=1} - 2\Gamma_{mn} |_{q=1}) \\ &+ h h_{,X_1} \sum_{n=0}^{N-2} -\sigma^2 \tilde{\eta}^{(0)} (k_{tr} T_n + 2k T_{n,(kh)} [kh]_{tr}) h^2 (g_m |_{q=1} G_n |_{q=1} - \Gamma_{mn} |_{q=1}) \\ &+ h h_{,X_1} \sum_{n=0}^{N-2} \sigma^2 k h T_n \tilde{\eta}^{(0)} [- (2g_m |_{q=1} G_n |_{q=1} - 2\Gamma_{mn} |_{q=1}) \\ &+ (g_m |_{q=1} R_n |_{q=1} - \Theta_{mn} |_{q=1}) - g_m |_{q=1} g_n |_{q=1} - \theta_{mn} |_{q=1} + 2\gamma_{mn} |_{q=1}] \\ &+ h h_{,X_1} g_m |_{q=1} (g \tilde{\eta}_{,h}^{(0)}), m = [0, N] \end{aligned} \quad (\text{A.14})$$

All $\tilde{\eta}_{,h}^{(0)}$ terms are then moved from the RHS to the LHS (as they are unknowns) and a linear matrix is then solved for $\tilde{\eta}_{,h}^{(0)}$ and $\tilde{u}_n^{(1)}$, $n = 0, 1, \dots, N$. When written in the form

$$\frac{\tilde{\eta}_{,h}^{(0)}}{\tilde{\eta}^{(0)}} = \frac{\gamma_h}{h} \quad (\text{A.15})$$

this may be compared to the linear Stokes solution (e.g. Madsen and Schäffer, 1998)

$$\gamma_h = - \frac{2(kh) \sinh 2(kh) + 2(kh)^2 (1 - \cosh 2(kh))}{(2(kh) + \sinh 2(kh))^2} \quad (\text{A.16})$$

B. Second Order Stokes Expansions

At second order of nonlinearity for a flat bed in one horizontal dimension, the mass equation becomes

$$\eta_{,t}^{(1)} + \sum_{n=0}^N \mu^{\beta_n} u_{n,x}^{(1)} h g_n |_{q=1} = -A_1 - \mu^2 A_2 \quad (\text{B.1})$$

where nonlinear forcing terms are

$$\begin{aligned} A_1 &= (u_0^{(0)} \eta^{(0)})_{,x} g_0 |_{q=1} \\ A_2 &= \sum_{n=1}^2 (u_n^{(0)} \eta^{(0)})_{,x} g_n |_{q=1} \end{aligned} \quad (\text{B.2})$$

Thus, inclusion of A_1 terms will produce $O(1)$ long wave nonlinearity (equivalent in order to Peregrine, 1967 and Nwogu, 1993), while the

addition of $\mu^2 A_2$ terms will produce nonlinearity equivalent in order to Wei et al. (1995). The weighted momentum equations are then

$$\begin{aligned} & \sum_{n=0}^N \mu^{\beta_n} u_{n,t}^{(1)} h \phi_{mn}|_{q=1} - \sum_{n=0}^{N-2} \mu^{\beta_{n+2}} u_{n,xt}^{(1)} h^3 (G_n g_m - \Gamma_{mn})|_{q=1} \\ & + g \eta_{,x}^{(1)} h g_m|_{q=1} \\ & = -B_1 - \mu^2 B_2, \quad m = [0, N] \end{aligned} \quad (B.3)$$

where similar remarks apply to the B_1 and $\mu^2 B_2$ terms,

$$\begin{aligned} B_1 &= u_{0,t}^{(0)} \eta^{(0)} g_m|_{q=1} + u_0^{(0)} u_{0,x}^{(0)} h g_m|_{q=1} + g \eta_{,x}^{(0)} \eta^{(0)} g_m|_{q=1} \\ B_2 &= \sum_{n=1}^2 \left[u_{n,t}^{(0)} \eta^{(0)} \phi_{mn} - u_n^{(0)} \eta_{,t}^{(0)} \varepsilon_{mn} \right] |_{q=1} \\ & + \sum_{n=1}^2 \left[\left(u_0^{(0)} u_n^{(0)} \right)_{,x} h \phi_{mn} - u_n^{(0)} u_{0,x}^{(0)} h \varepsilon_{mn} \right] |_{q=1} \\ & - \frac{3}{2} u_{0,xt}^{(0)} \eta^{(0)} h^2 (g_m - \nu_m)|_{q=1} - u_{0,xt}^{(0)} \eta_{,x}^{(0)} h^2 g_m|_{q=1} \\ & + \frac{h^3}{2} \left(\left(u_{0,x}^{(0)} \right)^2 - u_0^{(0)} u_{0,xx}^{(0)} \right)_{,x} (g_m - \nu_m)|_{q=1} \end{aligned} \quad (B.4)$$

At second order nonlinearity, surface elevations and velocities for steady waves have the form of a wave with the same phase speed but twice the wavenumber $\eta^{(1)} = \tilde{\eta}^{(1)} \exp(2i\psi) + c.c.$ and $u_n^{(1)} = \tilde{u}_n^{(1)} \exp(2i\psi) + c.c.$, where $\psi_x = k$, $\psi_t = -\sigma$ as before. Substitution of the first order linear wave solutions for surface elevation, frequency and orbital velocities into second order equations then gives the complete second order steady solution, for which we are most concerned with the bound second harmonic of surface elevation.

References

Abramowitz, M., Stegun, I.A., 1964. Handbook of Mathematical Functions. Dover Publications, New York . 1046 pp.
 Barthelemy, E., 2004. Nonlinear shallow water theories for coastal waves. Surveys in Geophysics 25, 315–337.
 Beji, S., Battjes, J.A., 1993. Experimental investigations of wave propagation over a bar. Coastal Engineering 19, 151–162.
 Beji, S., Battjes, J.A., 1994. Numerical simulation of nonlinear wave propagation over a bar. Coastal Engineering 23, 1–16.
 Bonneton, P., Barthelemy, E., Chazel, F., Cienfuegos, R., Lannes, D., Marche, F., Tissier, M., 2011a. Recent advances in Serre–Green–Naghdi modelling for wave transformation, breaking, and runup. European Journal of Mechanics B-Fluids 30, 589–597.
 Bonneton, P., Chazel, F., Lannes, D., Marche, F., Tissier, M., 2011b. A splitting approach for the fully nonlinear and weakly dispersive Green–Naghdi model. Journal of Comparative Physiology 230, 1479–1498.
 Chazel, F., Lannes, D., Marche, F., 2011. Numerical simulation of strongly nonlinear and dispersive waves using a Green–Naghdi Model. Journal of Scientific Computing 48, 105–116.
 Chen, Q., Kirby, J.T., Dalrymple, R.A., Kennedy, A.B., Chawla, A., 2000. Boussinesq modeling of wave transformation, breaking, and runup. II: 2D. Journal of the Waterways, Harbors and Coastal Engineering 126, 48–56.
 Chen, Y., Liu, P.L.-F., 1995. Modified Boussinesq equations and associated parabolic models for water wave propagation. Journal of Fluid Mechanics 288, 351–381.
 Dean, R.G., Dalrymple, R.A., 1991. Water Wave Mechanics for Engineers and Scientists. World Scientific Publishing Co., Singapore.
 Dingemans, M.W., 1994. MAST-G8M note, Rep. H1684, Delft Hydraulics. Comparison of computations with Boussinesq-like models and laboratory measurements.
 Ertekin, R.C., Webster, W.C., Wehausen, J.V., 1986. Waves caused by a moving disturbance in a shallow channel of finite width. Journal of Fluid Mechanics 169, 275–292.

Gobbi, M.F., Kirby, J.T., 1999. Wave evolution over submerged sills: tests of a high-order Boussinesq model. Coastal Engineering 37, 57–96 (and erratum, Coastal Eng. 40, 277).
 Gobbi, M.F.G., Kirby, J.T., Wei, G., 2000. A fully nonlinear Boussinesq model for surface waves. II. Extension to $O(\mu^4)$. J. Journal of Fluid Mechanics 405, 181–210.
 Green, A.E., Naghdi, P.M., 1976. A derivation of equations for wave propagation in water of variable depth. Journal of Fluid Mechanics 78, 237–246.
 Kennedy, A.B., Fenton, J.D., 1997. A fully nonlinear numerical method for wave propagation over topography. Coastal Engineering 32, 137–161.
 Kennedy, A.B., Chen, Q., Kirby, J.T., Dalrymple, R.A., 2000a. Boussinesq modeling of wave transformation, breaking, and runup. I: 1D. Journal of Waterway, Port, Coastal and Ocean Engineering 126, 39–47.
 Kennedy, A.B., Dalrymple, R.A., Kirby, J.T., Chen, Q., 2000b. Determination of inverse depths using direct Boussinesq modeling. Journal of Waterway, Port, Coastal and Ocean Engineering 126, 206–214.
 Kennedy, A.B., Kirby, J.T., Chen, Q., Dalrymple, R.A., 2001. Boussinesq-type equations with improved nonlinear performance. Wave Motion 33, 225–243.
 Kennedy, A.B., Kirby, J.T., 2002. Simplified higher-order Boussinesq equations – 1 Linear simplifications. Coastal Engineering 44, 205–229.
 Kim, J.W., Bai, K.J., Ertekin, R.C., Webster, W.C., 2003. A strongly-nonlinear model for water waves in water of variable depth – the irrotational Green–Naghdi model. Journal Offshore Mechanics Arctic Engineering 125, 25–32.
 Lannes, D., Bonneton, P., 2009. Derivation of asymptotic two-dimensional time-dependent equations for surface water wave propagation. Physics of Fluids 21, 016601 <http://dx.doi.org/10.1063/1.3053183>.
 Lynett, P.J., Wu, T.R., Liu, P.L.-F., 2002. Modeling wave runup with depth-integrated equations. Coastal Engineering 46, 89–107.
 Lynett, P.J., Liu, P.L.-F., 2004. A two-layer approach to wave modelling. Proceedings of the Royal Society B 460, 2637–2669.
 Madsen, O.S., Mei, C.C., 1969. Transformation of a solitary wave over an uneven bottom. Journal of Fluid Mechanics 39, 781–791.
 Madsen, P.A., Agnon, Y., 2003. Accuracy and convergence of velocity formulations for water waves in the framework of Boussinesq theory. Journal of Fluid Mechanics 477, 285–319.
 Madsen, P.A., Murray, R., Sørensen, O.R., 1991. A new form of the Boussinesq equations with improved linear dispersion characteristics. Part 1. Coastal Engineering 15, 371–388.
 Madsen, P.A., Sørensen, O.R., 1992. A new form of the Boussinesq equations with improved linear dispersion characteristics. Part 2. A slowly varying bathymetry. Coastal Engineering 18, 183–204.
 Madsen, P.A., Schäffer, H.A., 1998. Higher order Boussinesq-type equations for surface gravity waves – derivation and analysis. Philosophical Transactions of the Royal Society A 356, 1–59.
 Musumeci, R.E., Svendsen, I.A., Veeramony, J., 2005. The flow in the surf zone: a fully nonlinear Boussinesq-type of approach. Coastal Engineering 52, 565–598.
 Nwogu, O., 1993. Alternative form of Boussinesq equations for nearshore wave propagation. J. Journal of Waterway, Port, Coastal and Ocean Engineering 119, 618–638.
 Nwogu, O., Demirebilek, Z., 2010. Infragravity wave motions and runup over shallow fringing reefs. Journal of Waterway, Port, Coastal, and Ocean Engineering 136, 295–305.
 Peregrine, D.H., 1967. Long waves on a beach. Journal of Fluid Mechanics 27, 815–827.
 Schäffer, H.A., 2009. A fast convolution approach to the transformation of surface gravity waves: Linear waves in 1DH. Coastal Engineering 56, 517–533.
 Schäffer, H.A., Madsen, P.A., 1993. A Boussinesq model for waves breaking in shallow water. Coastal Engineering 20, 185–202.
 Serre, F., 1953. Contribution À l'étude des écoulements permanents et variables dans les canaux. La Houille Blanche 8, 374–388.
 Shields, J.J., Webster, W.C., 1988. On direct methods in water-wave theory. Journal of Fluid Mechanics 197, 171–199.
 Shen, C.Y., 2001. Constituent Boussinesq equations for waves and currents. Journal of Physical Oceanography 31, 850–859.
 Sørensen, O.R., Schäffer, H.A., Madsen, P.A., 1998. Surf zone dynamics simulated by a Boussinesq type model. III Wave-induced horizontal circulations. Coastal Engineering 33, 155–176.
 Veeramony, J., Svendsen, I.A., 2000. The flow in surf-zone waves. Coastal Engineering 39, 93–122.
 Wei, G., Kirby, J.T., Grilli, S.T., Subramanya, R., 1995. A fully nonlinear Boussinesq model for surface waves. I. Highly nonlinear, unsteady waves. Journal of Fluid Mechanics 294, 71–92.
 Witting, J.M., 1984. A unified model for the evolution of nonlinear water waves. Journal of Comparative Physiology 56, 203–236.